

AD-A046 083

UNITED TECHNOLOGIES CORP SUNNYVALE CALIF CHEMICAL SY--ETC F/G 21/8.2  
PHASE I. DESIGN AND ANALYSIS OF SHORT LENGTH SUPER HIPPO MOTOR --ETC(U)  
OCT 77 P R SCANNELL, W A STEPHEN F04611-77-C-0027

UNCLASSIFIED

CSD-2635-ITR

AFRPL-TR-77-58

NL

OF  
ADA  
046083



END  
DATE  
FILMED  
12-77  
DDC

AD A 046083

AFRPL-TR-77-58

CSD 2635-ITR

# PHASE I, DESIGN AND ANALYSIS OF SHORT LENGTH SUPER HIPPO MOTOR ASSEMBLY

P. R. Scannell  
W. A. Stephen  
Chemical Systems Division  
P.O. Box 358  
Sunnyvale, CA 94088

October 1977

Interim Technical Report for Period 4 April 1977 — 10 June 1977

APPROVED FOR PUBLIC RELEASE;  
DISTRIBUTION UNLIMITED

Prepared for

**Air Force Rocket Propulsion Laboratory  
Director of Science and Technology  
Air Force Systems Command  
Edwards Air Force Base, CA 93523**

AD NO. \_\_\_\_\_  
DDC FILE COPY

DDC  
RECEIVED  
NOV 4 1977  
RECEIVED  
B

19 REPORT DOCUMENTATION PAGE		READ INSTRUCTIONS BEFORE COMPLETING FORM	
18 1. REPORT NUMBER AFRPL-TR-77-58	2. GOVT ACCESSION NO.	14 3. RECIPIENT'S CATALOG NUMBER CSD-2635-ITR	
6 4. TITLE (and Subtitle) PHASE I, DESIGN AND ANALYSIS OF SHORT LENGTH SUPER HIPPO MOTOR ASSEMBLY.		9 5. TYPE OF REPORT & PERIOD COVERED Interim Technical Rept. 4 Apr 77 to 10 June 77	
		6. PERFORMING ORG. REPORT NUMBER 2635-B004	
10 7. AUTHOR(s) P. R./Scannell W. A./Stephen		15 8. CONTRACT OR GRANT NUMBER(s) FO4611-77-C-0027	
9. PERFORMING ORGANIZATION NAME AND ADDRESS Chemical Systems Division United Technologies Corp. P.O. Box 358, Sunnyvale, CA 94088		16 10. PROGRAM ELEMENT, PROJECT, TASK AREA & WORK UNIT NUMBERS JON 505909JW 11/77	
11. CONTROLLING OFFICE NAME AND ADDRESS Air Force Rocket Propulsion Laboratory Edwards Air Force Base, CA 93523	11	12. REPORT DATE October 1977	
		13. NUMBER OF PAGES 90	
14. MONITORING AGENCY NAME & ADDRESS (if different from Controlling Office) 12 104 p.		15. SECURITY CLASS. (of this report) Unclassified	
		15a. DECLASSIFICATION/DOWNGRADING SCHEDULE	
16. DISTRIBUTION STATEMENT (of this Report)  Approved for public release; distribution unlimited			
17. DISTRIBUTION STATEMENT (of the abstract entered in Block 20, if different from Report)  DDC RECEIVED NOV 4 1977 RECEIVED B			
18. SUPPLEMENTARY NOTES			
19. KEY WORDS (Continue on reverse side if necessary and identify by block number)  HIPPO motor Ballistic test motor Nozzles			
20. ABSTRACT (Continue on reverse side if necessary and identify by block number)  The short length Super HIPPO motor is a single cartridge version of the Super HIPPO high pressure ballistic test motor. The motor operates at pressures to 2,500 psi with propellant charge weights to 24,500 lb and is used to test rocket motor nozzles and components. This report summarizes the design and analysis activities, phase I, of a contract to design, fabricate, and install at AFRPL. ←			

374 927

## NOTICES

When U.S. Government drawings, specifications, or other data are used for any purpose other than a definitely related government procurement operation, the Government thereby incurs no responsibility nor any obligation whatsoever, and the fact that the Government may have formulated, furnished or in any way supplied the said drawings, specifications or other data, is not to be regarded by implication or otherwise, or in any manner licensing the holder or any other person or corporation, or conveying any rights or permission to manufacture, use, or sell any patented inventions that may in any way be related thereto.

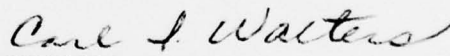
## FOREWORD

This report was submitted by United Technologies/Chemical Systems Division, P.O. Box 358, Sunnyvale, CA 94088, under Contract No. F04611-77-C-0027, Job Order No. 305909JW with the Air Force Rocket Propulsion Laboratory, Edwards AFB, CA 93523.

This report has been reviewed by the Information Office/DOZ and is releasable to the National Technical Information Service (NTIS). At NTIS it will be available to the general public, including foreign nations. This technical report has been reviewed and is approved for publication; it is classified and suitable for general public release.

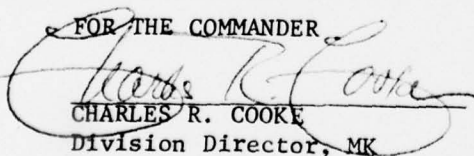


THOMAS L. KINSEL  
Project Manager



CARL I. WALTERS, Maj, USAF  
Branch Chief

FOR THE COMMANDER



CHARLES R. COOKE  
Division Director, MK

CONTENTS

Section	Page
1.0 INTRODUCTION	6
2.0 SHORT LENGTH SUPER HIPPO DESIGN DESCRIPTION	7
2.1 Motor Design Description	7
2.2 Design and Analysis Actions	12
3.0 DRAWING NUMBERS AND COMMONALITY WITH SUPER HIPPO AND ELSH	17
4.0 PERFROMANCE AND CAPABILITIES	19
5.0 STRESS, STRAIN ANALYSES, FACTORS OF SAFETY - SLSH	23
5.1 Introduction	23
5.2 Summary of Results and Conclusions	23
5.3 Structural Design Criteria	23
5.4 Material Properties	23
5.5 Method of Analysis	28
6.0 SHEAR KEY DESIGN	29
7.0 ACOUSTIC MODES OF SLSH MOTOR COMBUSTION	31
8.0 THERMAL ANALYSIS - INSULATION, FORWARD AFT, CARTRIDGE, AND NOZZLE ADAPTER	33
8.1 Introduction	33
8.2 Summary of Results	33
8.3 Description of the Analysis	35
8.3.1 Rubber Insulation Components	35
8.3.2 Aft Closure Asbestos-Phenolic Insulation	40
9.0 THERMAL ANALYSIS - GAP HEATING	41
10.0 TEST BAY INSULATION	47
11.0 GRAIN MEAN BULK TEMPERATURE	48
12.0 PHILOSOPHY OF RECYCLE OF INSULATION	51
12.1 Adapter Insulator	51
12.2 Aft Closure	51
12.3 Cartridge	51
12.4 Cartridge Spacer	52
12.5 Forward Insulator	52
12.6 Case Wall Insulation	52

ACCESSION for	
NTIS	<input checked="" type="checkbox"/>
DDC	<input type="checkbox"/>
ADDITIONAL	<input type="checkbox"/>
JUSTIFICATION	<input type="checkbox"/>
BY _____	
DISTRIBUTION/AVAILABILITY STATEMENTS	
Dist.	AVAIL. and/or
A	

CONTENTS (Continued)

Section		Page
13.0	HANDLING OF SLSH MOTOR COMPONENTS	53
	13.1 Forward Closure (Weight ~18,000 lb)	53
	13.2 Case (Weight ~13,000 lb)	53
	13.3 Aft Closure (Weight ~19,000 lb)	54
	13.4 Propellant Cartridge (Weight to 28,000 lb)	54
	13.5 Miscellaneous	54
	APPENDIX A: Thrust Stand Stress Analysis	56
	APPENDIX B: Super HIPPO Drawing List	58
	APPENDIX C: Stress Analysis Results	63
	APPENDIX D: Shear Key Sector Tests	78
	APPENDIX E: RPL Procedure for Lifting Super HIPPO Propellant Grains	88
	Abbreviations	91

## ILLUSTRATIONS

Figure		Page
2-1	SLSH Motor Assembly	8
4-1	SLSH Duration as Chamber Pressure for Various Throat Diameters, 23,000-lb Propellant	19
4-2	SLSH Thrust Time Capability	20
4-3	Ballistic Prediction for First SLSH Test	20
4-4	Ballistic Prediction for First SLSH Test	21
5-1	Super HIPPO Forward Closure LI65ZZZ Computer Model	25
5-2	Super HIPPO Aft Closure LI65ZZZ Computer Model (Input)	25
5-3	Super HIPPO Case LI65ZZZ Computer Model (Input)	25
5-4	Super HIPPO Aft Closure Deformed Outline (Computer Output)	25
5-5	Super HIPPO Aft Closure Stress Component (Computer Output)	26
5-6	HIPPO Forward Closure Deformed Outline (Computer Output)	26
5-7	Super HIPPO Forward Closure Stress Component (Computer Output)	26
5-8	Super HIPPO Case Deformed Outline (Computer Output)	27
5-9	Super HIPPO Case Stress Component (Computer Output)	27
8-1	Insulation Analysis Stations for IUS SLSH Cartridge	34
8-2	SLSH Asbestos-Phenolic Aft Closure	36
8-3	Ablation Rate Scaleup Due to Propellant Flame Temperature	39
9-1	IUS Super HIPPO Chamber Pressure History (1 mil/sec Throat Erosion, 70°F)	41
9-2	Steel Temperature Response - Case 2 (2% Chamber Pressure Oscillation, 200 Hz)	44
9-3	Case 3 - Steel Temperature Response (Aft Seal Gone/ Flowthrough)	45
9-4	Case 3 - SLSH Grain $\Delta P$ vs Time	46

ILLUSTRATIONS (Continued)

Figure		Page
11-1	Propellant Grain Mean Bulk Temperature vs Time for 70° Grain Exposed to 82° Mean Daily Temperature	49
11-2	Propellant Grain Mean Bulk Temperature vs Time for 70° Grain Exposed to 99° Mean Daily Temperature	50



TABLES

Table		Page
2-1	O-Ring Dimensions	16
3-1	Drawing List, Weights, Commonality	18
4-1	Predicted Performance	22
5-1	Summary of Margins of Safety	24
8-1	IUS Super HIPPO Cartridge	35
8-2	Internal Insulation Ablation Rate Prediction for IUS	37

## 1.0 INTRODUCTION

This report summarizes the design and analysis conducted in phase I of contract No. F04611-77-C-0027 during the period 7 April 1977 to 10 June 1977. The overall objective of this program is to design, fabricate, and deliver to AFRPL a single-cartridge Super HIPPO type test motor capable of testing large-scale nozzles at pressure levels up to 2,500 psi with propellant capacity to 24,500 lb. The addition of this motor to the Super HIPPO system will provide the capability for efficient and realistic testing of components for upper stages of the next generation of ballistic missiles and launch vehicles.

The short length Super HIPPO (SLSH) completes the family of Super HIPPO workhorse test motors at AFRPL. The existing Super HIPPO motor has a 46,000-lb propellant capacity and the existing extended length Super HIPPO (ELSH) has an 89,000-lb propellant capacity. All three motors are of the same size and use interchangeable parts.

## 2.0 SHORT LENGTH SUPER HIPPO DESIGN DESCRIPTION

### 2.1 MOTOR DESIGN DESCRIPTION

The motor is a single propellant cartridge version of the Super HIPPO motor assembly as shown in CSD drawing C12413 and figure 2-1. The motor design is the same as that of the Super HIPPO and ELSH in that the case consists of a cylindrical barrel with flat plate end closures attached by double clevis pin joints. The motor case is approximately half the length of the Super HIPPO case to accommodate one cartridge-loaded propellant grain. The shear key attachments for nozzles or nozzle adapters are the same design as previously used on Super HIPPO and ELSH. The forward and aft insulators are the same as used on the Super HIPPO but with increased thickness on the rubber portion of the forward insulator to be compatible with the longer duration tests contemplated. The motor is ignited with a single C00631-07-01 igniter suspended into the propellant bore through the nozzle throat. The motor is capable of assembly using Super HIPPO/ELSH propellant grains. The motor case mates with and uses the existing Super HIPPO closures, insulation, cartridges, and seals, and is compatible with the following items:

<u>Part No.</u>	<u>Item</u>
C10120-01-01	Aft closure
C10277-XX-01	Forward insulation
C10280-01-01	Aft insulation
C10141-01-01	Straight pin
C10278-01-01	Spacer
C11479-0X-01	Loaded cartridge (typical)

The motor developed on this program does not include propellant grains, igniters, nozzles, or insulated nozzle adapters. However, these items are shown on the SLSH-IUS motor assembly drawing to provide a medium for defining installation requirements and to provide a motor assembly drawing for use with the IUS nozzle for the first motor test. An alternate SLSH motor assembly excludes the insulated nozzle adapter and nozzle.

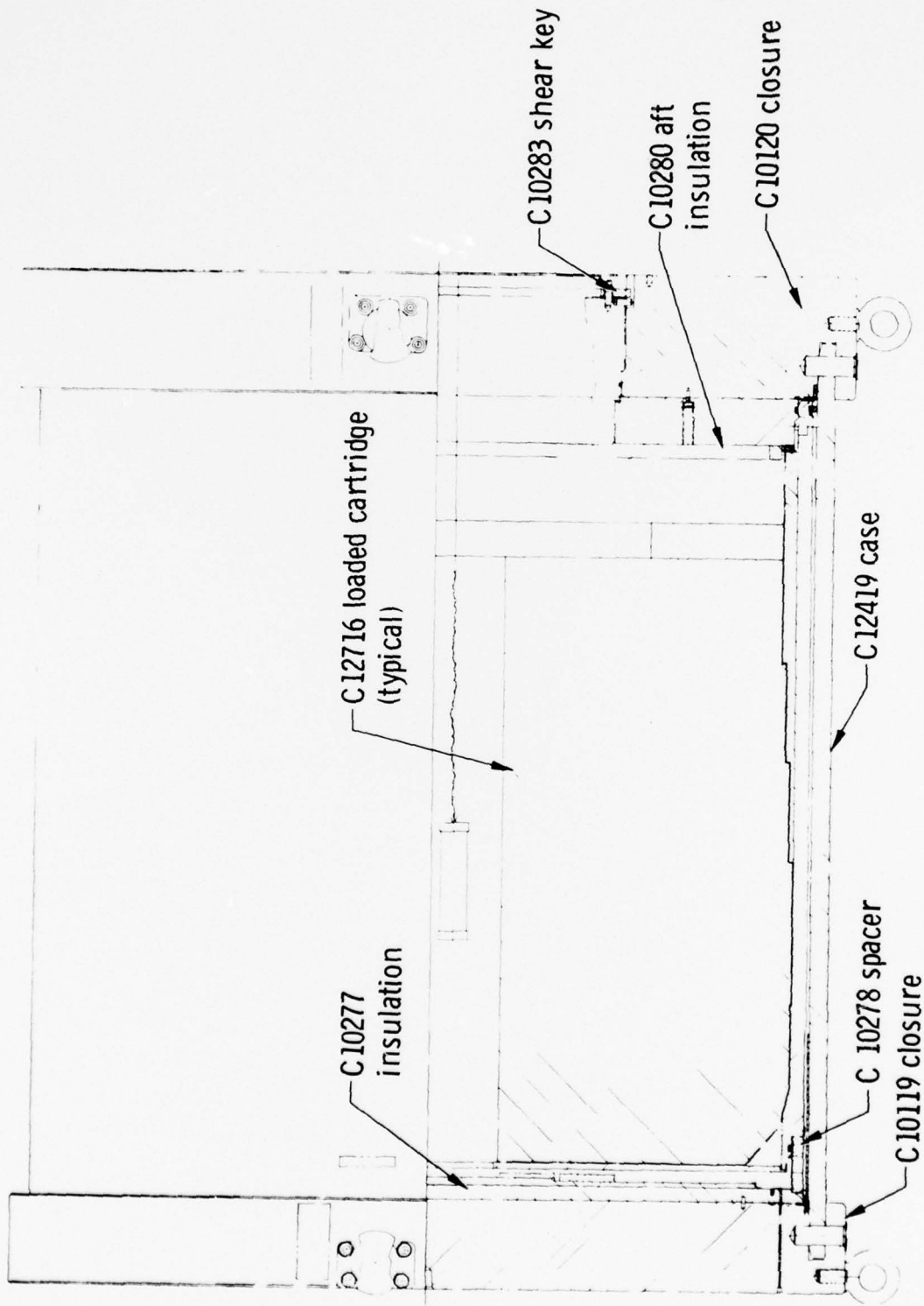


Figure 2-1. SL5H Motor Assembly

11659

The motor case is compatible with existing Super HIPPO handling equipment. The motor case is made of Government-furnished HY130 steel and designed for a 5,000-psig burst strength and 2,500-psig MEOP with a safety factor of 2. The motor is capable of operating for 145 sec at 1,000 psi. The motor is adaptable to mounting to the Super HIPPO thrust stand or bolting to a simple thrust support.

The Super HIPPO propellant grain will fit directly into the case. The pressurization of the cavity outboard of the propellant grain cartridge works exactly as on Super HIPPO and ELSH; the gases flow under the propellant cartridge, through the holes in the C10278 spacer, and up along the walls. The O-ring seal between the aft insulator and the top of the propellant cartridge prevents through-flow of hot gases along the steel wall. The pressure drop down the propellant grain is considerably lower with this motor than with Super HIPPO or ELSH, so that there is less pressure drop behind the cartridge to cause a through-flow.

The motor insulation is made primarily of two materials, a hard asbestos phenolic material and silica-asbestos loaded Buna-N rubber (NBR). The asbestos phenolic is used for the aft insulator, the basic forward insulator, and the insulation plugs. The aft insulator bolts onto the closure, and the phenolic material is specified to provide structural stiffness. Similarly, the phenolic part of the forward insulator is held down by the weight of the propellant grains. The forward insulator also centers the bottom of the propellant grains in the motor case. A pin in the forward closure centers the forward insulator, and the grains center on a shoulder on the insulator. The insulation plugs protect the bolts which secure the insulation to the aft closure and they are retained by threads in the aft insulation. While not a part of this contract, the nozzle adapter is being made of the same asbestos phenolic material and retained by similar bolts which are protected by similar insulation plugs. The interface between the adapter insulator and the aft closure insulator contains a stagger joint so that direct radiation to the steel from the combustion gases is avoided. The stagger joint contains a cavity for placement of zinc chromate putty to control charging by hot gases.

The rubber insulation is used in areas where structural requirements of the insulation are for flexibility rather than for stiffness. The design of the rubber parts specifies tolerances wide enough to essentially eliminate machining. The parts can be laid up of green rubber sheets, cured, inspected, and shipped. Four rubber insulation items are used in addition to the forward restrictor and sidewall rubber of the cartridges: the forward insulator discs, the forward insulator blocks, the case wall insulation, and the aft insulator ring.

The forward insulator rubber discs are secured to the phenolic part of the forward insulator by a double-faced tape and protect the phenolic part. Thickness of rubber required depends on the pressure, duration, and temperatures expected. The design height of the cartridge above the forward insulator phenolic portion will accept 3/4-in.-thick rubber with an additional thickness in the center port. The considerations are that (1) the char and erosion will be much deeper where the forward restrictor of the cartridge does not protect from the direct radiation from the core of combustion gases (i.e., under the grain the char and erosion will be lower); and (2) sufficient flow area must be provided between the forward restrictor of the grain and the forward insulator to allow flow of combustion gases for charging the cavity between the cartridge and case wall. The minimum flow area is defined by the product of the length of the inside perimeter of the restrictor and the vertical clearance from that perimeter to the forward insulator. Note that 1-1/2 in. of asbestos phenolic underlies the rubber sheet to protect the forward closure, so that underestimating the thickness of rubber required would not be catastrophic. The insulation was analyzed for 145-sec duration capability.

Rubber blocks are positioned and bonded on the forward insulator in a radial array to provide support for the forward insulator late in the firing after the grain has burned back and no longer supports the restrictor. The purpose is to keep the restrictor from sagging down onto the forward insulator, thereby sealing off the flow passage for charging gases into the cavity surrounding the propellant cartridge. These blocks were reduced in thickness from 1-in. on Super HIPPO/ELSH to 3/4-in. to allow greater forward insulator rubber thickness.

The gases which charge the cavity between the cartridge and the case would tend to impinge the steel case wall where they flow through the holes in the spacer, so a 1/4-in.-thick sheet of rubber is bonded to the inside of the case in this zone. The outside of the Super HIPPO propellant cartridge is reduced in diameter over the lower 18 in. to allow flow area for the gases in the region where this rubber sheet is installed. The nominal clearance between the case and cartridge is 0.2 in. unpressurized to allow for machining tolerances on these 7-ft-diameter components. This is identical to the Super HIPPO and ELSH and similar analysis applies. Above the 18-in.-wide rubber sheet, a coat of DC 93-104 rubber is applied and cured in place. Thickness of this coating was increased to 1/8 in. for the long duration test.

The fourth item of rubber insulation is a rectangular cross-section ring bonded to the inner face of the aft insulator near the outer perimeter. This ring provides protection from thermal radiation for the region of the O-ring which seals between the cartridge and the aft insulator. The insulation was designed for multiple cycle capability at 1,500-psi/40-sec duration operation in the Super HIPPO, and for 1,400 psi/60-sec duration in the ELSH. Approximately 1/4-in. of insulation was consumed from the surfaces of the forward and aft insulators during 40 sec at 1,500 psi with high combustion temperatures on the Super HIPPO demonstration test. Up to 1 in. of ablative material could thereby be charred and/or eroded in a 145-sec duration test, but only in those areas exposed to direct radiation from the core of the combustion gases. On the forward insulator, the rubber sheets are designed to be consumed each test and to protect the more expensive asbestos phenolic part which has accurate machining requirements. The 145-sec test would require 3/4 in. of insulation extending under the grain plus an extra 1/4-in. thickness in the center. One such rubber disc is being fabricated on this contract for the long duration test. In addition, a 1/4-in. rubber disc will be provided to stack with a C10277-13-01 forward insulator to form a second long duration insulator. A number of rubber insulators (C10277-12-01 and C10277-13-01) were provided under the Super HIPPO contract. These are 1/2-in. thick, and item -13 has an additional 1/4-in. disc in the center. Between use of available new Super HIPPO forward insulator parts and

refurbishment with V-61 between tests, no other forward insulator parts should be required for five motor tests.

One forward insulator phenolic part is being fabricated to be reused for the five tests indicated.

The aft insulator, at 5.16 in. thick, provides ample insulation capacity for tests of 145-sec duration at 1,000 psi. However, one test at 145-sec duration and four tests at 60-sec duration would require two aft insulators. One aft insulator is being fabricated as negotiated.

The new forward closure is being made to the C10119 drawing using 4340 steel heat treated to a minimum ultimate strength of 125,000 psi. The closure will be fully interchangeable with the existing Super HIPPO/ELSH C10119 forward closure with the exception of two new threaded holes which were added to the design for securing the closure to the SLSH thrustmount.

The IUS project nozzle adapter shown on drawing C12411 will physically fit the same nozzles as the CHAR motor flange; 4340 steel was specified for the adapter and the design was analyzed for 5,000-psi burst capability. The hydrotest drawing provides for a configuration for testing the IUS/CHAR nozzle adapter, and a suitable hydroflange was designed and analyzed (C12416). No provision was made for fabricating this flange or bolts under this contract.

## 2.2 DESIGN AND ANALYSIS ACTIONS

Ten new drawings or new configurations and analyses were required for the SLSH motor.

- A. The short barrel motor case design (C12419) is identical to the existing design for the Super HIPPO case except that the length is reduced by the maximum stacking length of one propellant grain, 81.19 in. The tolerance on the case length was reduced from the Super HIPPO version because closer dimensional control is possible with the shorter motor. The case length was also reduced by the amount of tolerance reduction.



The material for the case is Government-furnished HY130 steel as used in the Super HIPPO and ELSH motor cases. The structural analysis performed for the earlier cases is adequate and rigorous to this program. This analysis consists of a finite element computer analysis of the Super HIPPO case and the interactions of the case and closures.

- B. The forward closure is interchangeable with the existing Super HIPPO forward closure and will be made to the same drawing (C10119). ECOs were issued to add tapped holes to the closure for attaching to a thrust mount for motor operation external to the Super HIPPO thrust stand. New structural analysis consisted only of confirming the structural adequacy of the closure to accept the additional holes. The Super HIPPO analysis is rigorous and applicable.
- C. The shear key is the C10283-03-01 shear key used on the Super HIPPO demonstration test. This shear key has been pressure tested to 1,800 psi with blocked throat. This is equivalent to approximately 1,900 psi with the IUS nozzle flowing. Since the IUS MEOP is 1,000 psi, this is a demonstrated safety factor of 1.9. No drawings or ECOs are required.
- D. A hydrostatic proof test flange (C12416) was designed for use on the CHAR nozzle flange to provide for the 3,750-psi hydrotest. The material is 4340 steel. Fill and bleed ports through the flange have 1-1/4-in. AND threads on the outside face and 1-1/2-in. pipe threads for a stand pipe on the inside face, as on the Super HIPPO. Use of a 1-1/2 in. internal stand pipe for fill and empty will allow rapid removal of the water after the hydrotest. The aft face of the flange will also be drilled and tapped for lifting eyes. Structural analysis was performed by manual techniques due to the large margins of safety. This item has been designed but is not authorized for fabrication on this contract.

- E. The basic forward insulator design will be the same as that used on Super HIPPO (C10277). This insulator consists of a lower asbestos phenolic portion which centers on a probe in the center of the forward closure and extends under the spacer which supports the cartridge. This part has accurate machining and flatness requirements and is fairly expensive. It is intended to be reused five or ten times, depending on test duration. The phenolic insulator is protected by a consumable rubber sheet insulator with no accurate machining requirements. The rubber part of the insulator is 1/2-in. thick for the Super HIPPO demonstration test of 40 sec at 1,500 psi. The rubber part of the ELSH unit is 3/4-in. thick at the center for 60 sec at 1,400 psi. The portion of the rubber under the shadow of the forward propellant grain can be much thinner. For this motor, additional configurations of insulator were added to the drawing: one that is 1-in. thick in the center and 3/4-in. thick further out, and one that is 1/4-in. thick over the full diameter to space up existing -13 insulators (ELSH) to 1-in. thick at the center. Also, a design change was added to allow fabricating the phenolic portion in two pieces, a small disc and a concentric ring. No structural analysis is contemplated.
- F. A hydrotest assembly drawing (C12420) was prepared similar to the Super HIPPO hydro assembly (C10286) with configurations for testing with the solid shear key, the notched shear key, and the IUS adapter. No new detailed analysis is contemplated, as the Super HIPPO analysis applies. The adapter was analyzed under the IUS program.
- G. An alternate hydrotest assembly lists only SLSH components and excludes IUS unique parts.
- H. A loaded motor assembly drawing (C12411) was prepared essentially the same as Super HIPPO motor assembly C11167 but with the single-cartridge configuration and specifying the IUS nozzle, adapter,

and grain. Analysis consisted of review and update of the gap charging analysis and thermal analysis for firing 140 sec at 1,000 psi.

- I. An alternate loaded assembly excludes the IUS insulated adapter and nozzle. While this is a general purpose workhorse motor, the insulation design assumes a forward restrictor, particularly beyond the 72-in. diameter. Any grain design which is not restricted on the forward face outboard of 50-in. diameter should be reviewed carefully.
  
- J. The O-ring dimensions were standardized by use of common ID dimensions for close sizes and making the cross-section tolerances alike. Three sizes were deleted, leaving seven sizes (plus smaller standard units). The -1 is already obsolete, and the -3 and -5 sizes will now be dropped. IDs will be standardized at 83.0/82.5, 78.5/78.0, 40.10/39.98, and 55.22/55.10 in. Cross-sections will be 0.515/0.485 in. in 90, 70, and 50 durometer, 0.575/0.545 in. in 70 durometer, and 0.289/0.269 in 70 durometer (Shore A). The sizes are shown in table 2-1.
  
- K. A new thrust mount was designed for fabrication by the AFRPL weld shop. It has 3-in.-thick upper and lower plates and the uprights are welded of 2-in. plate. The design is intended to assume overloads to 10,000,000 lb should a closure fail. It should also have some lateral capability should a nozzle fail asymmetrically. As designed, the lateral capability of the stand will accept the original Super HIPPO lateral force requirement of 81,000 lb when in combination with 300,000-lb axial force readily with the short length motor, marginally with the Super HIPPO motor. The limiting condition is the bolts holding the forward closure to the stand which are assumed to be 170,000-psi UTS Allen bolts. The 12 studs (1-1/4-7) into the concrete should be 90 ksi to provide equivalent strength.

See Appendix A for the stress analysis.

TABLE 2-1. O-RING DIMENSIONS

T2151

No.	Test, lb	ID, in.	Cross- section	Shore A	Super HIPPO Quantity	ELSH Quantity	SLSH Quantity
C10144-10-01	35	78.5/78.0	0.515/0.485	50	1	1	1
C10144-09-01	35	83.0/82.5	0.575/0.545	70	2	3	2
C10144-08-01	35	83.0/82.5	0.515/0.485	90	2	3	2
C10144-07-01	15	55.22/55.10	0.289/0.269	70	-	1	-
C10144-06-01	35	78.5/78.0	0.515/0.485	70	3	7	2
C10144-04-01	15	40.10/39/98	0.289/0.269	70	1	-	1
C10144-02-01	15	78.5/78.0	0.289/0.269	70	3	3	3

NOTES:

In application, the -05s are replaced by -06s, the -03 is replaced by -02, and -01 is obsolete.

The use of only four ID values allows a simple layout board for controlling length (diameter) of all seven sizes for butt joining O-rings of linear stock.

In addition, color coding was added to mark 90 durometer stock red and 50 durometer stock yellow.

### 3.0 DRAWING NUMBERS AND COMMONALITY WITH SUPER HIPPO AND ELSH

Table 3-1 lists quantities of items supplied under this contract for the SLSH motor and indicates commonality of usage for Super HIPPO and ELSH testing. A complete list of Super HIPPO, ELSH, and SLSH drawings is included as Appendix B.

TABLE 3-1. DRAWING LIST, WEIGHTS, COMMONALITY

T2152

Quantity	Part Number	Description	Common to Super HIPPO	Common to ELSH	Weight, lb
1 ea	C12419-01-01	Short Super HIPPO motor case	No	No	13,200
1 ea	C10277-11-01	Forward insulation - phenolic	X	X	700
1 ea	C10280-01-01	Aft insulation - phenolic	X	No(a)	1,400
1 ea	C10144-02-01	O-ring	X	X	1
1 ea	C10144-04-01	O-ring	X	No(a)	1
2 ea	C10144-05-01	O-ring	X	X	3
2 ea	C10144-08-01	O-ring	X	X	4
2 ea	C10144-09-01	O-ring	X	X	3
1 ea	C10144-10-01	O-ring	X	X	3
2 ea	C10142-01-01	O-ring retainer (set) 222351	X	X	21
120 ea	C10141-01-01	Straight pin 224570	X	X	6
1 ea	C10119-01-01	Forward closure	X	X	18,000
1 ea	C11167-14-01	Rubber (ring on aft insulation)	X	X	30
6 ea	C11167-12-01	Rubber blocks	X	X	1
1 ea	C10277-14-01	Forward rubber insulation	X	X	400
1 ea	C10277-15-01	Forward rubber insulation	X	X	150
(b) 1 ea	C10120-01-01	Aft closure	X	No(a)	19,000
2 ea	C10289-0X-0X	Trunnions	X	X	90
24 ea	C10276-01-01	Plug, insulation aft	X	X	0.3
16 ea	AN960-1616	Washer, flat	X	X	-
24 ea	AN960-616	Washer, flat	X	X	-
72 ea	MS51960-67	Screw	X	X	-
16 ea	NAS 1351-16-14	Screw	X	X	-
24 ea	AN6-10	Screw	X	X	-
32 ea	MS21250-12016	Bolt	X	No(a)	-
4	C11199-01-01	Ring, centering (each)	X	X	3
32 ea	WC-12	Washer	X	No(a)	-
1 gal	MIL-G-4343	O-ring lub	X	X	-
1 can	MIL-T-5544	Thread lub	X	X	-
2	1 1/2 - 6	Eye bolt	X	X	-
1	C11167-11-01	Rubber case insulation set	X	X	-
1 gal	EA 913	Adhesive	X	X	-
10 rolls	---	Putty, zinc chromate, 1-in. wide	X	X	-
2 rolls	Scotch 425	Foil tape	X	X	-
15 rolls	Scotch 890	Glass reinforced tape	X	X	-
10 gal	No. 11 Wax 2	Cement	X	X	-
7 lb	DC 93-104	Silicone rubber	X	X	-
1 gal	DC 36060	Primer	X	X	-
2 rolls	Devoseal 7565	Double-coated tape?	X	X	-
2 ea	PD 2493	Shipping box for clevis pins	X	X	-
1 gal	Lockbond No. 55	Solvent for No. 11 wax 2	X	X	-
(c) 1 ea	C10278-01-01	Spacer			110
(c) 1 ea	C10295-01-01	Or equivalent cartridge			26,000
(c) 1 ea	C00631-07-01	Igniter			2
(c) 1 ea	C12592-01-01	Or equivalent nozzle adapter			2,200
(c) 1 ea	C12590-01-01	Or equivalent adapter insulator			
(c) 1 ea	C12416-01-01	Hydroplug			1,100

(a) Items associated with aft closure could be used with small nozzle

(b) Use existing Super HIPPO item

(c) Provided by using program

#### 4.0 PERFORMANCE AND CAPABILITIES

Figure 4-1 shows the duration capability of various nozzles from 4- to 20-in. throat. Capacities using CHAR grains are about 85% of those shown. The very short and the very long durations are difficult to obtain because of burning rate limitations (0.2 to 1.5 in./sec at 1,000 psi) of available propellants. Capacity of the CHAR end burner would be 90% of the values shown. As a practical matter, a star grain of some manner would be recommended to test with the very large nozzles at high thrust so that conventional propellants would be used. This would reduce capacity somewhat.

Figure 4-2 shows thrust time capability for a single Super HIPPO grain with a maximum charge, using an optimum nozzle. Capabilities for some typical reduced charges are also shown.

Figures 4-3 and 4-4 show ballistic predictions for the first SLSH test with the IUS nozzle and propellant grain. Table 4-1 summarizes ballistic performance predictions for the IUS/SLSH.

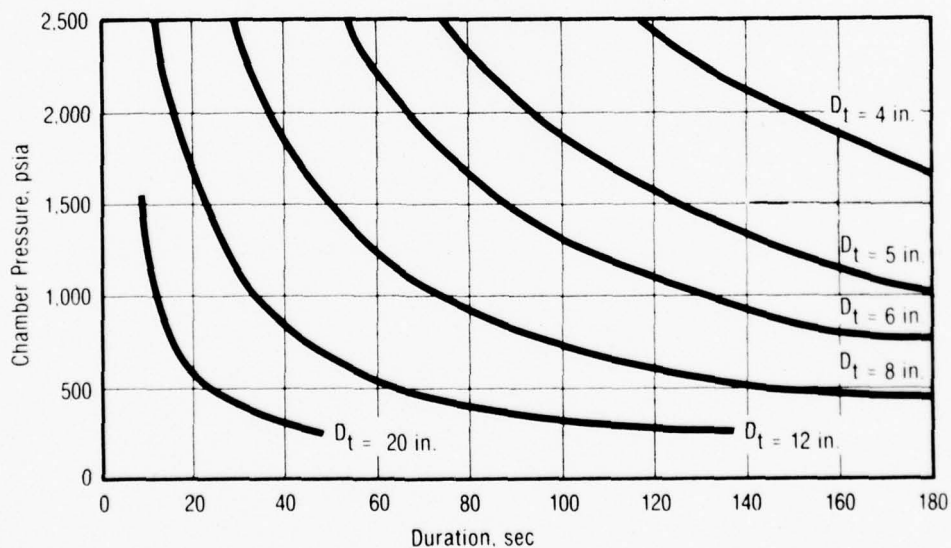


Figure 4-1. SLSH Duration as Chamber Pressure for Various Throat Diameters, 23,000-lb Propellant

10163

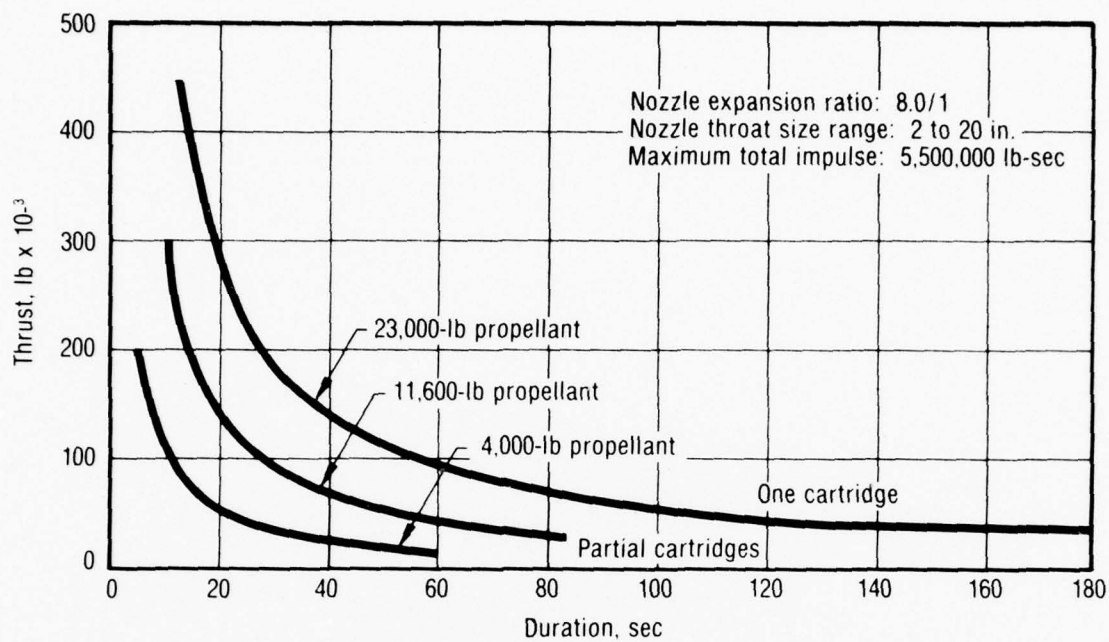


Figure 4-2. SLSH Thrust Time Capability

10164

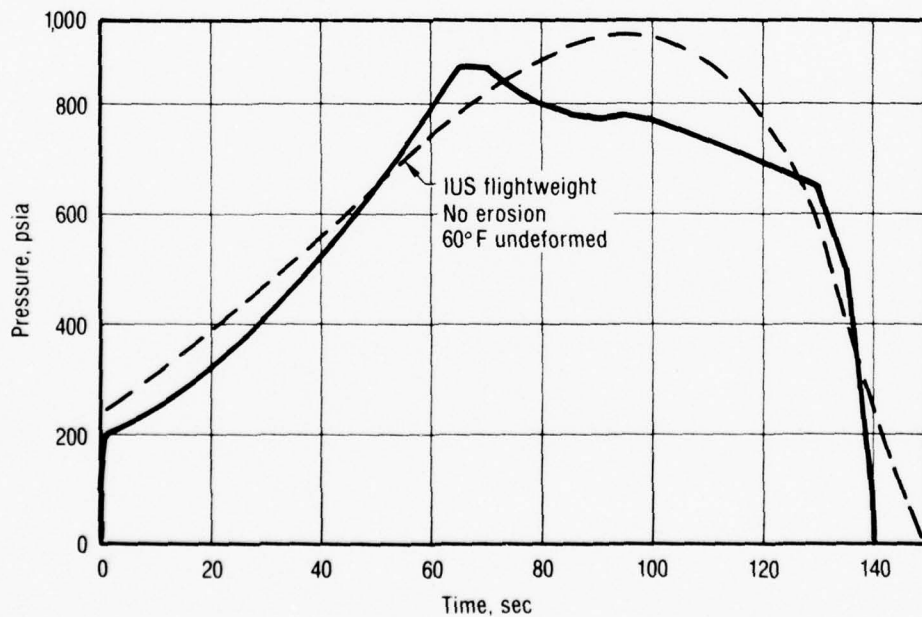


Figure 4-3. Ballistic Prediction for First SLSH Test

11660



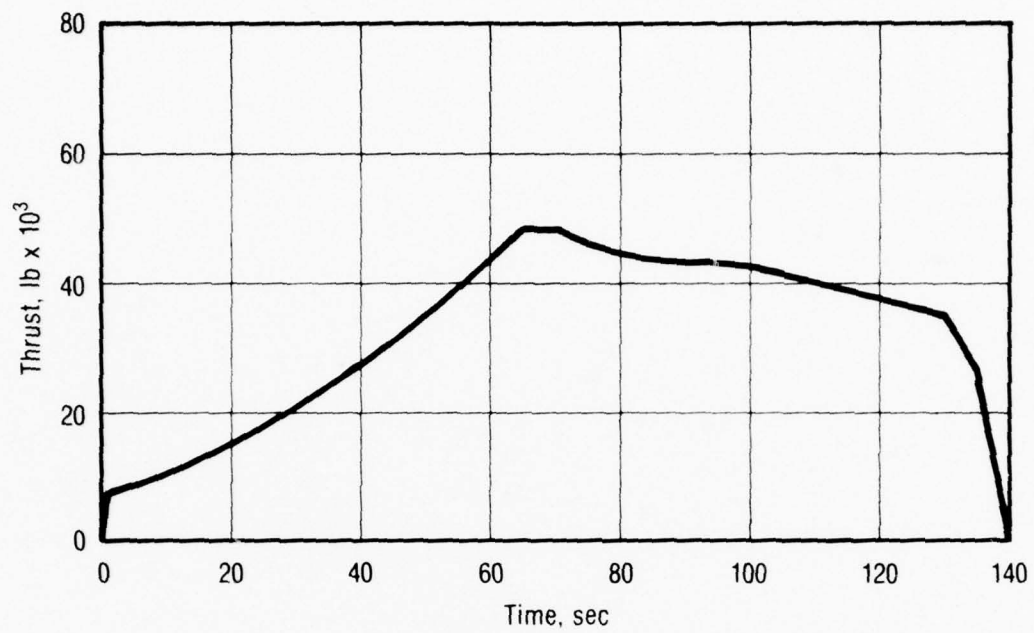


Figure 4-4. Ballistic Prediction for First SLSH Test

11661

TABLE 4-1. PREDICTED PERFORMANCE  
FIRST SLSH TEST

T2153

<u>Assumption</u>	<u>Value</u>	
Propellant	UTP-19,360	
Burning rate at 600 psia, in./sec	0.237	
Pressure exponent	0.41	
Propellant weight, lb	19,949	
Propellant density, lb/in. <sup>3</sup>	0.0635	
Characteristic velocity, ft/sec	5,000	
Initial throat diameter, in.	6.825	
Expansion ratio	8.0	
Nozzle efficiency	0.95	
Gamma	1.14	
Bore diameter, in.	15.5	
Grain length, in.	66	
Predicted Performance	<u>1 Mil/Sec Erosion</u>	<u>No Throat Erosion</u>
Web time, sec	143.4	139.3
Web time average chamber pressure, psia	564	608
Maximum chamber pressure, psia	818	869
Duration, sec	144.0	140.1

## 5.0 STRESS, STRAIN ANALYSES, FACTORS OF SAFETY - SLSH

### 5.1 INTRODUCTION

Presented in this section is the structural analysis of the SLSH case components. This analysis demonstrates the structural adequacy for the ultimate design pressure of 5,000 psi. The structural components analyzed were the case, forward plate, aft plate, aft plate to nozzle adaption, case pins, and aft plate keys.

### 5.2 SUMMARY OF RESULTS AND CONCLUSIONS

The critical stresses and corresponding margins of safety are summarized in table 5-1. The finite element models, deformed outline, and stress contour plots are shown in figures 5-1 through 5-9.

The results of the structural analysis show the Super HIPPO components are capable of withstanding the imposed structural load without structural failure.

### 5.3 STRUCTURAL DESIGN CRITERIA

The chamber maximum operating pressure (MEOP) used in the structural analysis was  $P_{MEOP} = 2,500$  psi. All results are for an ultimate pressure (PULT) of 5,000 psi based on a safety factor of two times the MEOP.

The margins of safety reported are based on the comparison of maximum uniaxial ultimate stress with the design allowable uniaxial material ultimate strengths.

### 5.4 MATERIAL PROPERTIES

The material properties used are summarized below:

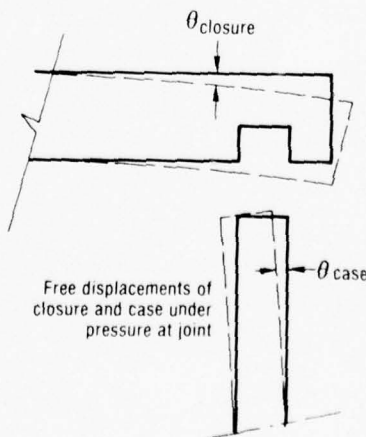
- A. Case (HY130)
  - $F_{TU} = 140,000$
  - $F_{TY} = 130,000$
  - $F_{SU} = 87,600$

TABLE 5-1. SUMMARY OF MARGINS OF SAFETY

T2154

<u>Item</u>	<u>Mode</u>	<u>Stress, ksi</u>	<u>Margin of Safety</u>
Forward plate	Hoop stress	115	+0.08
	Plate Bending		
Aft plate	Hoop stress	105	+0.19
	Plate Bending		
Case	Hoop stress	134	0.04
	Axial Stress	165 <sup>a</sup>	>0.4
	Edge tear-out	71	Plastic +0.2
Pin	Shear	100	+1.0
	Moment	142	Plastic
Key	Shear	53	+1.0
	Bending	153	+0.2
	Bolts	158	+0.1

a Elastic - The closure and the case rotate in opposite directions at the joint as shown below. Finite element runs were made on each to determine the rotation due to moment applied at the pins. From these runs, the moment was determined that gave compatibility of displacement. This moment gave an axial stress of 165,000 psi at the surface of the case. A plastic analysis was made where the elements with a stress above the yield stress (130,000 psi) were allowed to deform and transfer the load into the adjacent material. This run showed there was a substantial plastic margin for the ultimate load condition. The yield area is shown in figure 5-9; it should be noted that the resulting deformations are so small that they will have no effect on the function of the structure.



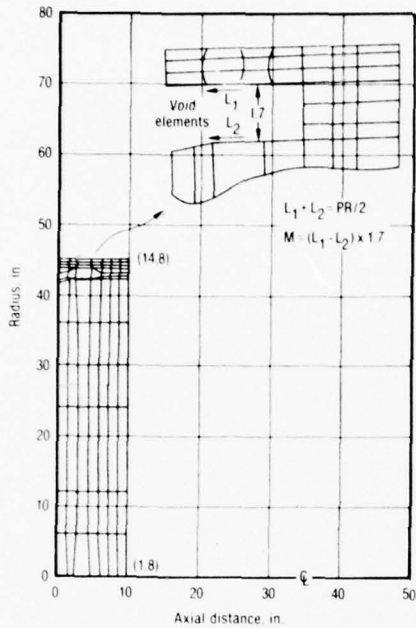


Figure 5-1. Super HIPPO Forward Closure LI65ZZZ Computer Model

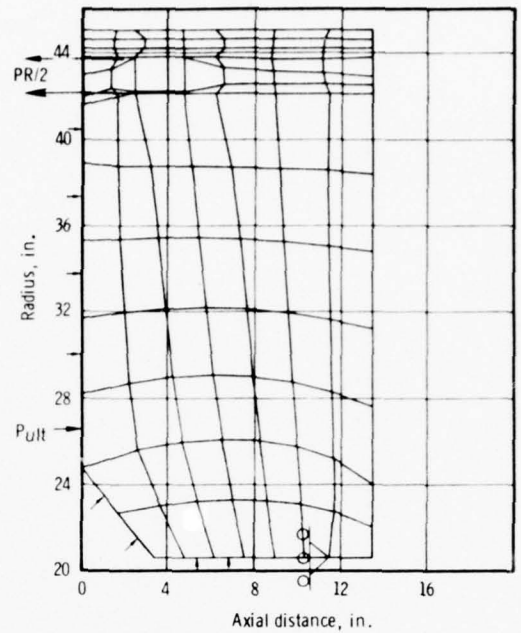


Figure 5-2. Super HIPPO Aft Closure LI65ZZZ Computer Model (Input)

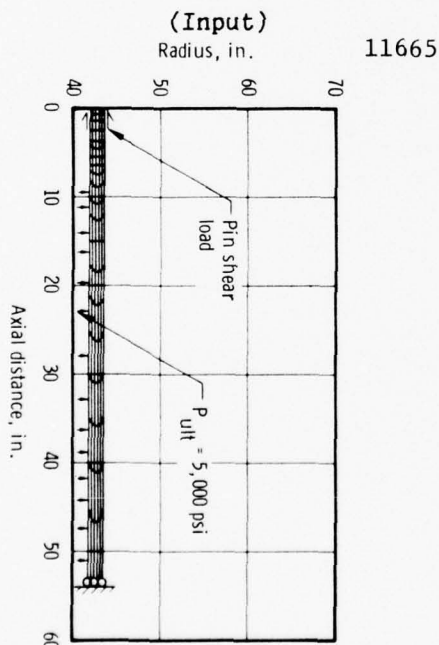


Figure 5-3. Super HIPPO Case LI65ZZZ Computer Model

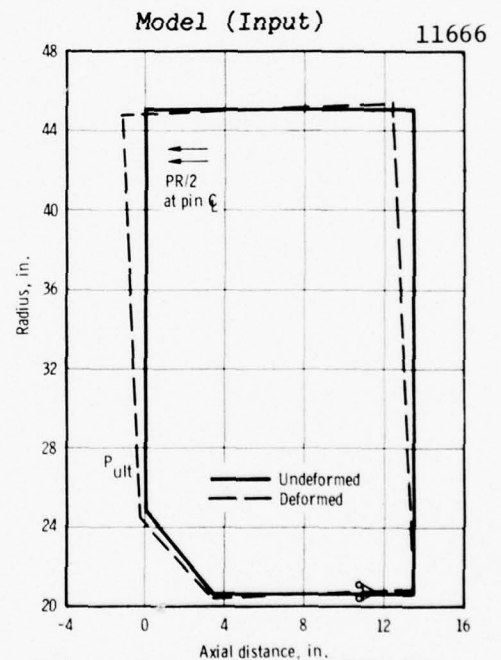


Figure 5-4. Super HIPPO Aft Closure Deformed Outline (Computer Output)

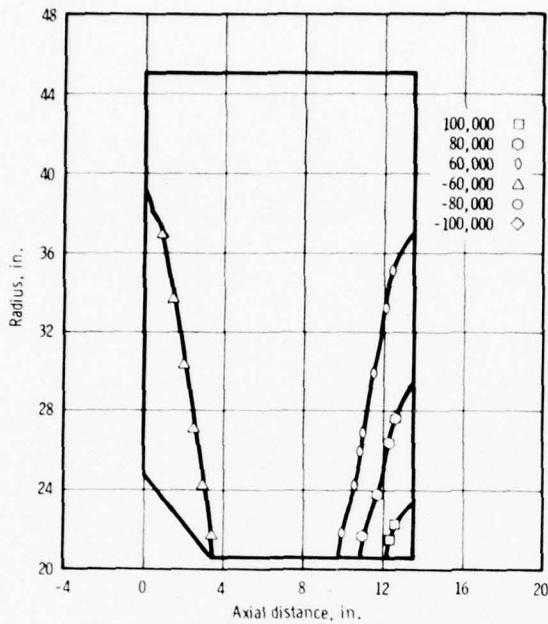


Figure 5-5. Super HIPPO Aft Closure Stress Component (Computer Output) 11669

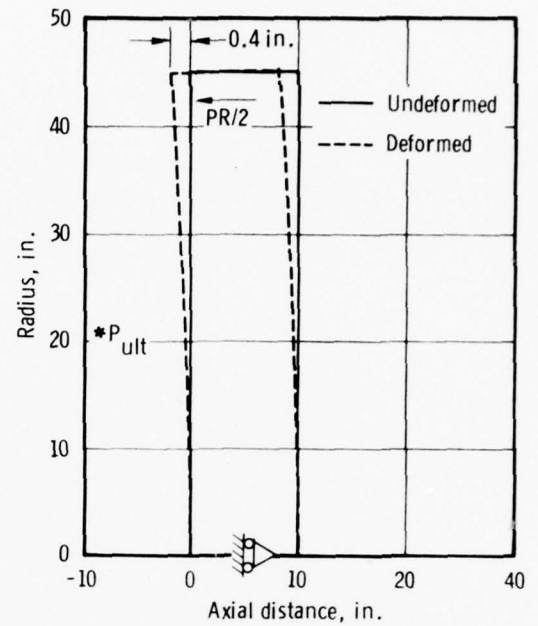


Figure 5-6. HIPPO Forward Closure Deformed Outline (Computer Output) 11670

$$F_{BRU} = 230,000$$

$$E = 30 \times 10^6$$

B. Closure and Adapter (4340 steel per MIL-S-5000, Cond. E)

$$F_{TU} = 125,000$$

$$F_{TY} = 103,000$$

$$F_{SU} = 82,000$$

$$F_{BRU} = 194,000$$

$$E = 29 \times 10^6$$

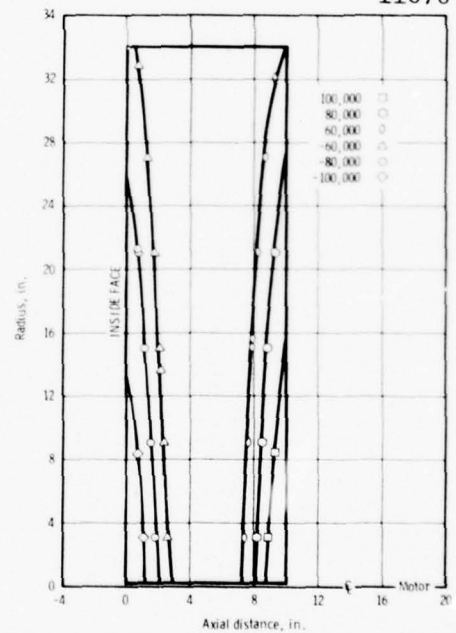


Figure 5-7. Super HIPPO Forward Closure Stress Component (Computer Output) 11671

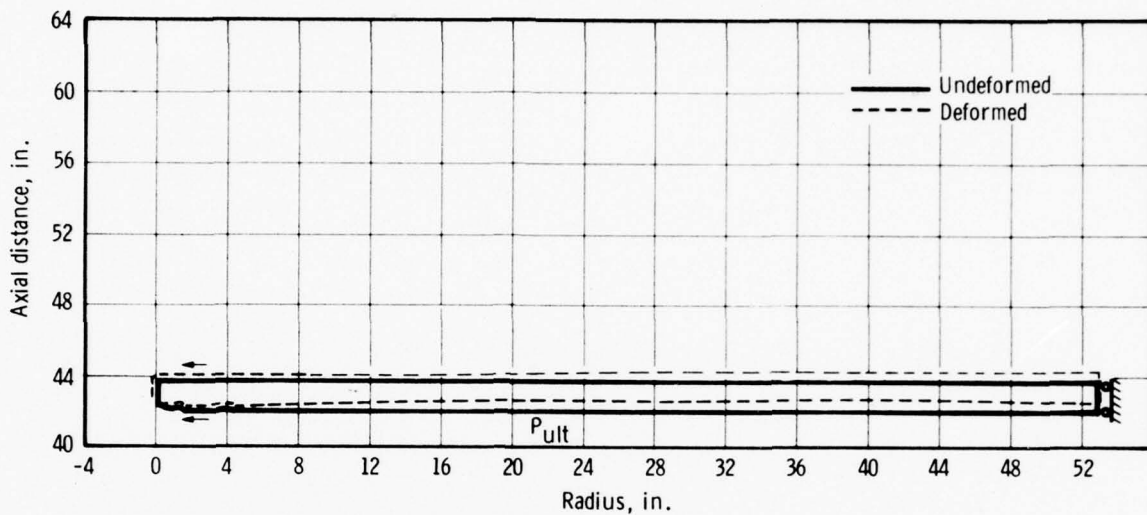


Figure 5-8. Super HIPPO Case Deformed Outline  
(Computer Output)

11672

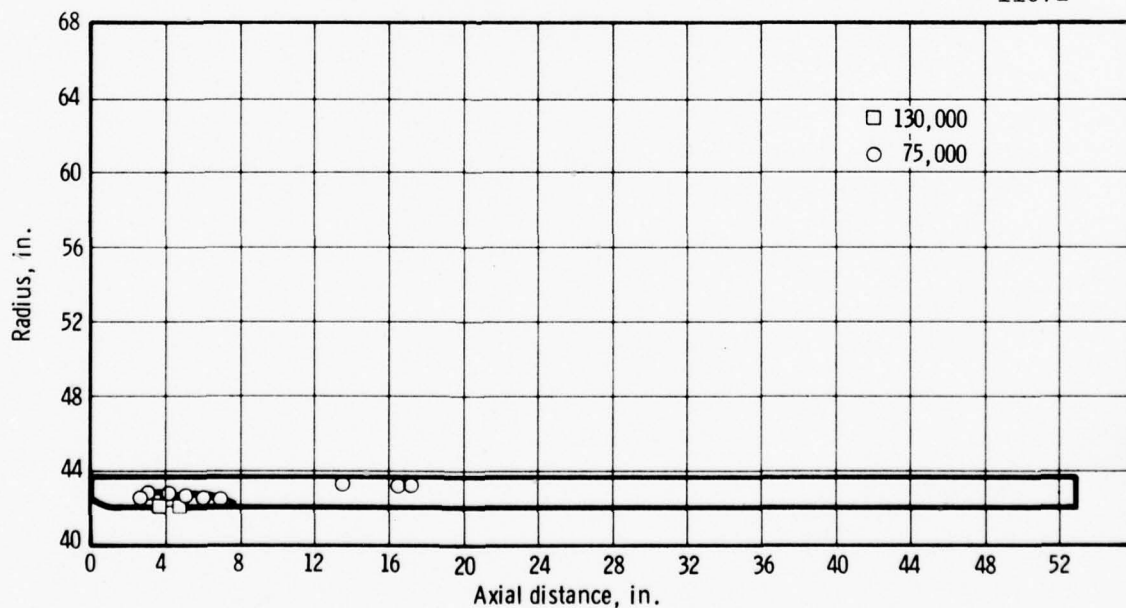


Figure 5-9. Super HIPPO Case Stress Component  
(Computer Output)

11673

C. Pins and Keys (4340 steel per MIL-S-5000, heat treated to 40 to 45 Rc)

$F_{TU} = 180,000$

$F_{TY} = 163,000$

$F_{SU} = 109,000$

$F_{BRU} = 250,000$

$E = 29 \times 10^6$

#### 5.5 METHOD OF ANALYSIS

The stresses were calculated using stress analysis computer program LI65ZZZ. This finite element stress analysis program determines stresses and displacements in complex elastic bodies of revolution isotropic material properties. The computer output consists of radial, tangential, axial, and shear stresses for each element and nodal displacements. The finite element representations used are shown in figures 5-1 through 5-4. Margins of safety are calculated for the metal parts comparing ultimate stresses with the material allowable stress. Margins of safety is defined as  $MS = (\text{allowable stress/ultimate stress}) - 1$ .

The results of these calculations are summarized in appendix C.



## 6.0 SHEAR KEY DESIGN

The function of the shear key is to protect the motor case from failure by overpressure by failing at a low enough pressure to vent the gases in the motor case before case deformation becomes excessive. A shear key can be either general-purpose or for a specific test. A general-purpose key must not fail below the contractual MEOP of the motor of 2,500 psi. However, if a specific test were to have a considerably lower MEOP (e.g., 1,000 psi as on the IUS/SLSH test), the shear key could be allowed to fail at a much lower pressure (e.g., 1,500 psi). In any event, the key must fail at a low enough pressure to allow the nozzle-adapter assembly to accelerate out of the aft closure far enough to generate a gas flow area between the adapter and the closure. Since the closure is 13-in. thick and the insulator is 5-in. thick, the assembly must travel 18-in. before an appreciable area is generated. Presumably, whatever caused the case pressure to increase to the failure pressure of the key will cause continued pressure increase until this additional flow area is developed. Thus, the maximum pressure at which the shear key releases must be considerably below the 5,000-psi burst of the case to provide protection. The nature of the shear key is such that the force or pressure at failure cannot be predicted very accurately. The key is not loaded in shear, but in a combination of shear and bending. The amount of rotation and bending depends on the accuracy of machining, installation and on wear. The properties of the metal are also subject to variation. For these reasons, model tests were conducted on contract No. F04611-72-C-0023 (appendix D). Based on these tests, the C10283-03-01 was designed for use on the Super HIPPO demonstration test firing with an MEOP of 1,700 psi and an average throat diameter of 12-1/2 in. Analysis of the data from the shear key testing indicated that the 3-sigma lowest pressure at which this shear key would fail was 2,550 psi and the 3-sigma highest pressure was about 4,000 psi.

The IUS/SLSH motor assembly design specifies reuse of this same shear key for key test firing. At equal chamber pressures, the forces on the key are higher with the IUS nozzle ( $d_t = 7$  in.) than with the demonstration test nozzle because of the smaller nozzle and thrust. The force on the

shear key is equal to chamber pressure acting over the area of the closure to adapter seal ( $P_c A_a$ ) minus thrust of the nozzle ( $P_c A_t C_f$ )

$$(F = P_c A_a - P_c A_t C_f = P_c (A_a - A_t C_f))$$

The ratio of force on the key with the IUS nozzle to that with the demonstration nozzle is:

$$R = \frac{F_{IUS}}{F_{demo}} = \frac{(A_a - A_{t_{IUS}} C_{f_{IUS}})}{(A_a - A_{t_{demo}} C_{f_{demo}})}$$

$$R = \frac{(40.6)^2 - (7)^2 (1.65)}{(40.6)^2 - (12.5)^2 (1.65)} = \frac{1567}{1390} = 1.127$$

Since the force on the shear key is higher for the same chamber pressure, the key will fail at a lower pressure. The theoretical lowest failure pressure is  $2,550/1.127 = 2,260$  psi. The theoretical highest failure pressure is  $4,000/1.27 = 3,550$  psi.

This shear key was hydrotested to 1,800 psi with a blind flange (i.e., no thrust). The force on the key during this hydrotest was higher than with the IUS nozzle flowing by the ratio  $R = (40.6)^2 / [(40.6)^2 - (7)^2 (1.65)] = 1.05$ .

The equivalent IUS firing pressure was  $(1.05) 1,800 = 1,890$  psi. The MEOP of the IUS test is 1,000 psi. Thus, a factor of safety of 1.89 has been demonstrated and the nozzle will not release inadvertently during the firing.

## 7.0 ACOUSTIC MODES OF SLSH MOTOR COMBUSTION

Acoustic mode calculations were made on the SLSH motor for the ignition geometry. These calculations used a finite element NASTRAN model and are based on a sonic velocity of 41,200 in./sec. The calculations were limited to axial modes: no transverse oscillation effects were included. The frequencies of these modes are tabulated below.

<u>Mode Number</u>	<u>Frequency, Hz</u>
1	130.0
2	298.4
3	480.6
4	694.8
5	841.4
6	1,044.0

Examination of the acoustic pressure distributions shows that the cavities at both ends of the motor have a significant impact on the acoustic frequency. As the motor burns, their influence will diminish. Therefore, these frequencies will shift toward the classical organ pipe frequencies, i.e.,  $f = (41,200 n)/(2L)$  Hz. For the fundamental ( $n = 1$ ), this means the 130 Hz mode will approach 250 Hz. Hence, one can expect significant changes in the acoustic frequencies as the motor burns.

As far as the stand is concerned, it seems that little can be done to detune the stand frequencies from the motor acoustics. The large acoustic frequency changes will sweep across the stand frequency somewhere during the burn, no matter what the stand frequency is.

On the positive side, the chances of combustion instability driving the acoustics, and hence the stand, to destruction seem small. The acoustic driving of most aluminized HTPB propellants is low at these frequencies. The acoustic damping is usually sufficient to prevent these troubles.

The natural vibration frequencies are estimated at 150 Hz in lateral oscillation and 400 Hz in axial vibration. The amplitude expected is less than  $\pm 0.001$  so that no interaction is expected.

## 8.0 THERMAL ANALYSIS - INSULATION, FORWARD AFT, CARTRIDGE, AND NOZZLE ADAPTER

### 8.1 INTRODUCTION

This section summarizes the thermal analysis which has been performed on the design of the cartridge insulation and internal components exposed to the exhaust gas environment in the SLSH motor with the IUS static test aft closure. The objective of this analysis was to determine thermal adequacy of the designs and to estimate the number of possible reuses of each component. Components which were included in the analysis were the aft closure and nozzle adapter, asbestos phenolic insulators, the rubber protector in the forward closure, cartridge insulation, and the restrictors. All analysis results were computed using one-dimensional heat conduction models and all ablation predictions were derived by scaling available correlated test data.

### 8.2 SUMMARY OF RESULTS

The internal insulation analysis of the SLSH covers the items shown in figure 8-1 and labeled as stations A through F. The environment to which these components are exposed is that of the IUS propellant where the average pressure is about 600 psia, the duration about 144 sec, and the flame temperature is 5,584°F (propellant UTP-19,360). The results of the rubber insulation evaluation, stations A through E, are summarized in table 8-1 where the insulation initial thickness (nominal), exposed duration of the station, and ablated depth are reported. At stations C and D, an evaluation was made to determine the impact to the insulation on the cartridge if the aft restrictor were to debond at ignition. As indicated in the table, there is still adequate insulation material if that were to happen. The forward closure station (station E), in the middle of the closure, shows the lowest safety factor when considering only the rubber insulation. Since that rubber insulation covers 1.5 asbestos-phenolic insulation, there is no concern as to the adequacy of protection in that region. The ablation rate used for the rubber insulation is the maximum expected anywhere in the lightweight configuration and would, therefore, be conservative for this configuration due to the large area ratios of the SLSH cartridge.

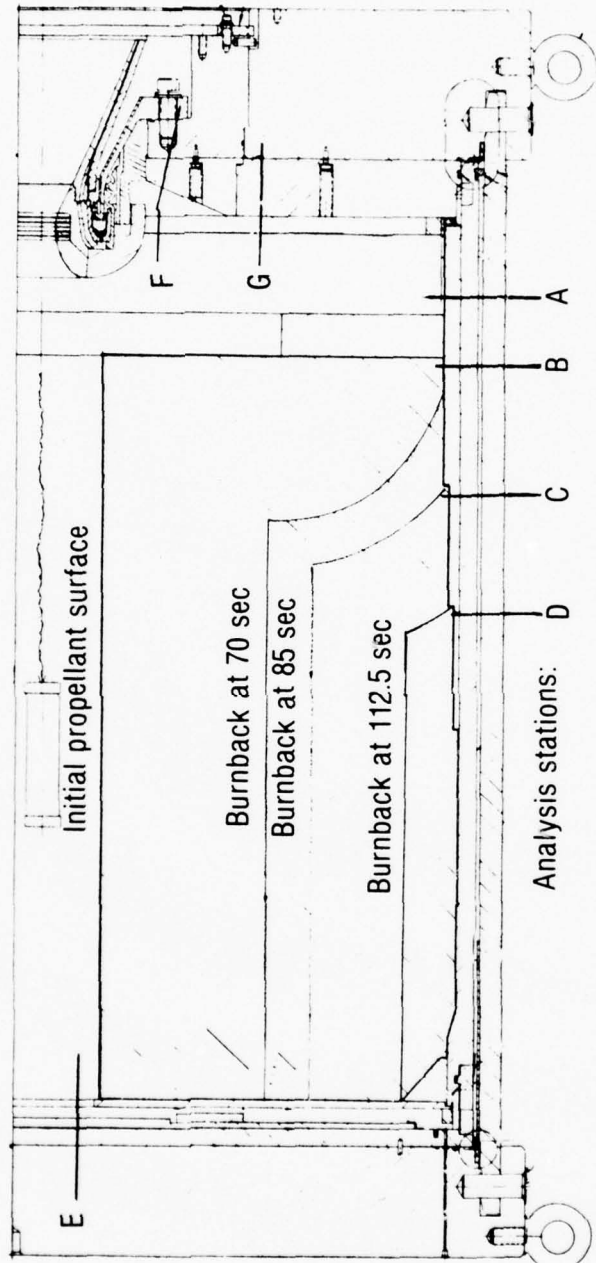


Figure 8-1. Insulation Analysis Stations for IUS SLSH Cartridge

11674

TABLE 8-1. IUS SUPER HIPPO CARTRIDGE

T2155

Ablation Rate = 5 mils/sec

Station	Initial Thickness, in.	Duration Exposed, sec	Ablated Depth, in.	Safety Factor
A	1.50	144	0.72	2.08
B	1.50	74	0.37	4.05
C	1.00	59	0.295	3.39
C <sup>a</sup>	1.00	87	0.435	2.30
D	0.50	31.5	0.158	3.17
D <sup>a</sup>	0.50	45	0.225	2.22
E <sup>b</sup>	1.0	144	0.72	1.39

<sup>a</sup> Worst case if aft inhibitor were to debond at ignition.

<sup>b</sup> Considering only the rubber portion of the insulation.

Stations F and G in the asbestos phenolic are shown to be adequate in figure 8-2, where the CMA heat conduction program was run to determine the char depths for motor burn and soakout. Multiple use of the aft closure insulator is demonstrated, while it is probable that only one use could be made of the nozzle adapter insulation.

Details of the analysis are described in the next section.

### 8.3 DESCRIPTION OF THE ANALYSIS

#### 8.3.1 Rubber Insulation Components

The ablation rate for the cartridge and forward closure rubber components is derived from the analysis conducted to determine the rates for the flight-weight IUS insulation. Table 8-2 lists the source of the ablation rate estimates for the IUS flightweight as determined from the C4 demonstration tests conducted at CSD under contract GL10A0120M/N003072C0108. The insulation for

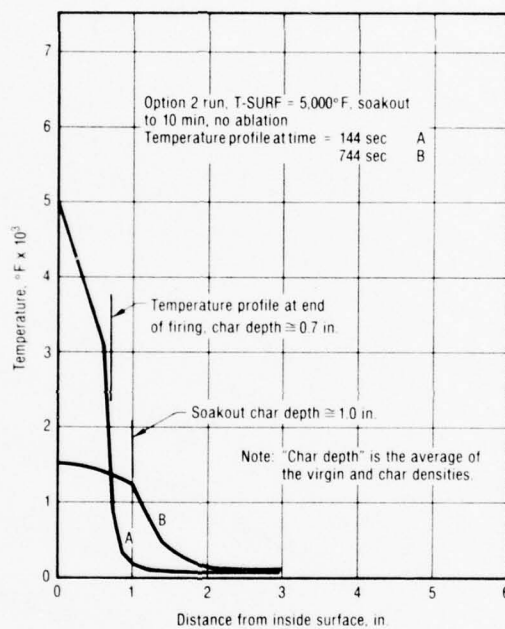


Figure 8-2. SL5H Asbestos-Phenolic Aft Closure

11675



TABLE 8-2. INTERNAL INSULATION ABLATION RATE PREDICTION FOR IUS

T2156

Data Base: C4 Demonstration Tests

Features Compared	IUS	C4 Demonstration
Pressure, psia	600	1,000
Flame temperature, °F	5,584	5,879
Duration, sec	144	44
Forward closure loaded	Yes	Yes
Aft recirculation zone	Yes	Yes
Nozzle submerged length/D*	3.52	2.5
Measured average ablation rate, mils/second		
Forward		5.42
Aft		6.0
Large area ratio		3.33
IUS predicted average ablation rate, mils/sec		
	<u>Initial analysis</u>	<u>Updated analysis</u>
Forward	4.6	4.42
Aft	5.2	5.00
Large area ratio	5.2	3.33

IUS flightweight motors is silica- and asbestos-loaded EPDM. For the Super HIPPO cartridges, the insulation is silica- and asbestos-loaded NBR rubber. The C4 large-scale and demonstration tests illustrated that the ablation rates for both types of rubber were approximately the same in the same environment. An examination of the "compared features" of the IUS and C4 motors in table 8-2 shows that the pressure and flame temperature are both less for IUS than for C4. In the areas of the rubber ablation, the radiation heat flux is significantly larger than the convective heat flux. As a result, it was conservatively determined that no scalings would be done due to pressure (which would be a convective heat flux correction), but a correction would be made for the radiation heat flux, since there was a significant difference in flame temperature.

To make the radiation correction, ablation data were required that could be considered to be primarily radiation caused. Figure 8-3 shows a curve of three data sets with such data. The lowest heat flux data are from the Titan III/C forward closure where there is no local propellant burning for over half of the firing (115 sec.). The next data point comes from the C4 large-scale test motors which had an unloaded forward closure (minimal convection), while the highest heat flux data come from the two-segment Super HIPPO check-out test, in the center of the forward closure. The IUS radiation heat flux level is indicated on the curve and represents a change in ablation rate of approximately 1 mil/sec. This heat flux is for the average chamber pressure of 600 psia where the temperature is 5,584°F. Therefore, for the forward and aft closure ablation data from the C4 demonstration motors, the rates were reduced by 1 mil/sec as shown in the updated analysis column. The ablation rates at the large area ratios were left unchanged since there was significant scatter to the data, and it was desirable to retain some amount of conservatism. It should be noted that the initial analysis had less of a radiation correction because it was conducted using the chamber temperature for a chamber pressure of 1,000 psia, slightly higher than that at 600 psia. The large area ratio data was also ignored.

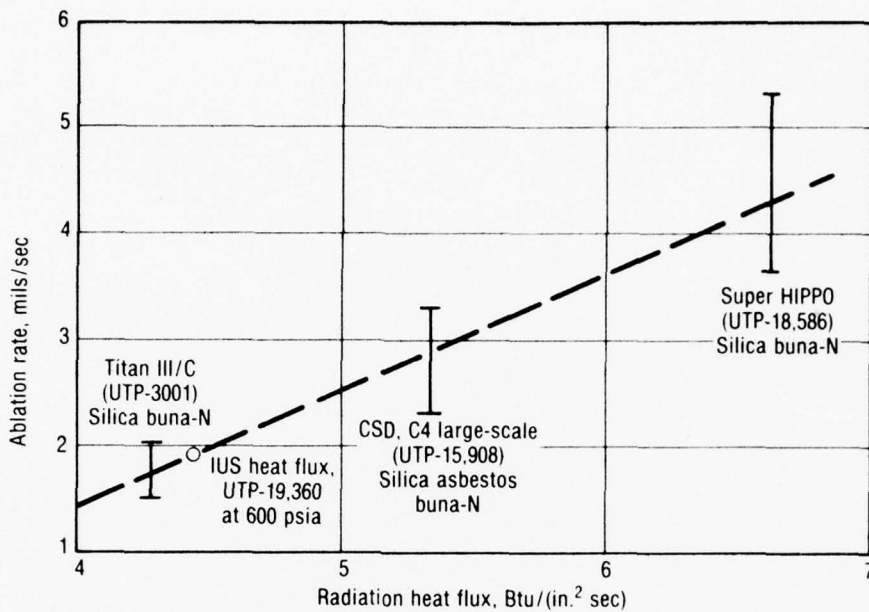


Figure 8-3. Ablation Rate Scaleup Due to Propellant Flame Temperature

11676

An examination of this ablation data was made, and it was decided that it would be conservative to use 5 mil/sec ablation rate for the SLSH IUS cartridge even though it would be considered large area ratio. When the 5-mil/sec rate is applied to the SLSH cartridge using the burnback data illustrated in figure 8-1, the ablation predictions in table 8-1 result.

The forward restrictor (1.5 in. thick), provides adequate protection since there is very little radiation heat transfer to the forward surface and the convection heat transfer is also small. In the aft end, the restrictor is a liner material, which typically may ablate on the order of 25 to 40 mils/sec. At 40 mils/sec for the necessary protection time of about 70 sec (2.8 in.), the 3.7 in. thick restrictor will provide adequate protection.

In the forward closure, the same 5 mil/sec ablation rate was applied to the center of the 1-in.-thick piece of rubber covering the asbestos phenolic. The safety factor of 1.39 provides adequate protection for the forward closure, especially since there is asbestos phenolic underneath.

### 8.3.2 Aft Closure Asbestos-Phenolic Insulation

Analysis stations G and F were evaluated with one CMA heat conduction run to show that there is sufficient material to protect the nozzle adapter and aft closure. As with the rubber insulation, the environment is primarily radiation, with a very small convection component. The current thermochemical boundary condition model with program ACE and CMA, which would normally provide sufficient data to conduct a transient thermochemical ablation and heat conduction analysis, does not function properly when the radiation level is significantly higher than the convection. Therefore, to simplify the analysis, it was assumed that the worst case (from a thermal penetration standpoint) would be where there were no ablation (no surface recession), but charring in-depth would take place. Therefore, a very conservative 5,000°F surface temperature was assigned to the surface of the CMA heat conduction model and it was run for 144 sec with 600 sec of soakout. This assumption is consistent with the measurements from the Super HIPPO checkout motor. The predicted char depths at burnout and soakout are shown on figure 8-2 and are 0.7 and 1 in., respectively. The results from the Super HIPPO checkout test showed that the char depth in the aft closure was 0.25 in. from the original surface of the asbestos phenolic. When this is scaled timewise from about 42 sec to 144 sec, the result is 0.82 in. of char. This is compatible with the CMA prediction shown in figure 8-2. The aft closure asbestos-phenolic insulator could, therefore, be used about three times for IUS length tests. It is assumed that the nozzle adapter insulator would be used only once.

## 9.0 THERMAL ANALYSIS - GAP HEATING

A charging and thermal analysis of the gap between the SLSH case and cartridge was conducted to quantify the case insulation requirements for a worst-case thermal environment. Hence, the chamber pressure history corresponding to the IUS Super HIPPO configuration as shown in figure 9-1, was used to size the DC 93-104 thickness so that case steel temperatures remain at acceptable levels for the duration of the firing. Based on the results of the first Super HIPPO firing, it was felt that adequate thermal protection is afforded the forward end of the case by the 0.25-in. insulator, hence, no analysis of this region was necessary. In addition, since any thermal damage to the OD of the cartridge can be easily accommodated with no adverse effects to the grain or case, no analysis of the cartridge was conducted. Thus, the gap analysis was primarily directed at the portion of the motor case just aft of the 0.25-in. insulator.

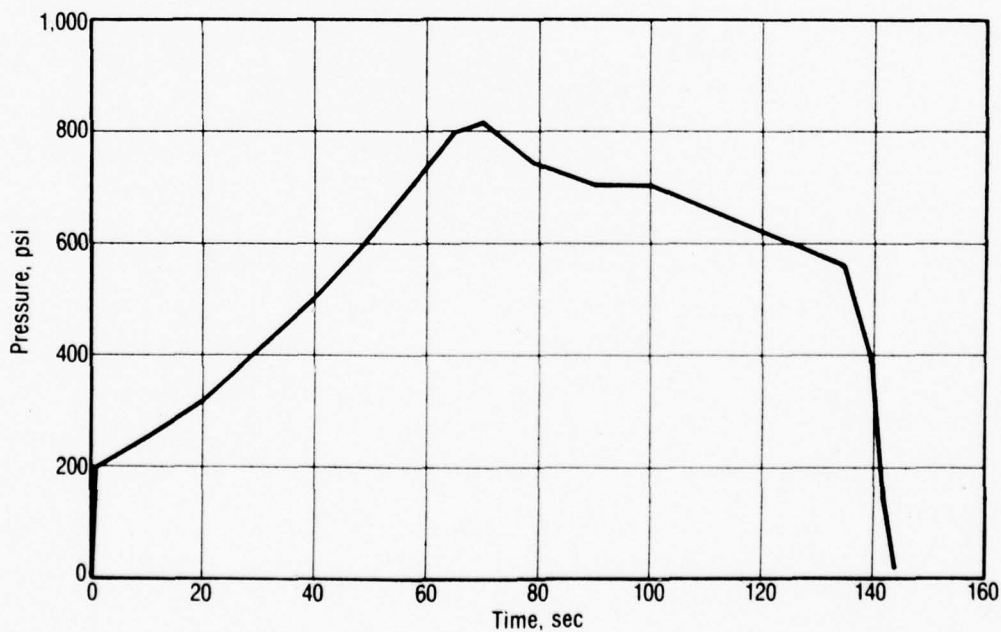


Figure 9-1. IUS Super HIPPO Chamber Pressure History  
(1 mil/sec Throat Erosion, 70°F)

11677

Three types of gap flow were examined; the first corresponded to a normal gap charging/cooldown, under the assumption that the aft seal remains intact and that no chamber pressure oscillations occur during the firing. This case, as one would expect, proves to be the least severe from a thermal standpoint. The second case involved the assumption of a normal gap charging to 0.5 sec, followed by a 200-Hz chamber pressure oscillation, with an amplitude equal to 2% of the nominal average chamber pressure of 600 psi, continuing throughout the firing duration. The third, and most severe case, assumes that failure of the aft seal occurs at ignition, resulting in a continuous flow through the gap driven by the grain  $\Delta P$ .

The main conclusion of the analysis is that 1/8 in. of DC 93-104 provides adequate thermal protection for the steel case for all three types of flow. A detailed summary of the analysis results and assumptions for each case follows.

#### SLSH Gap Heating Analysis

##### General Assumptions:

1. Chamber pressure history as shown in figure 9-1
2. Constant gap thickness = 0.25 in.
3. Analysis limited to one station just aft of 1/4-in. case insulator
4. Flame temperature gas assumed to enter gap through vent holes
5. Case OD assumed to be adiabatic surface for all runs.

Case 1: Nominal gap charging/cooldown, aft seal intact, no chamber pressure oscillations

##### Conclusions:

1. 0.125-in. DC 93-104 adequate to maintain steel temperatures below 100°F for duration of firing.

Assumptions:

1. Gap charging due to  $\Delta P$  between gap and chamber is essentially complete at 0.5 sec.
2. From 0.5 to 144 sec, additional filling of gap due to cooling-induced gap pressure drop assumed for a constant chamber pressure of 600 psi.
3. Heat transfer coefficients for initial charging (0 to 0.5 sec) calculated for flow between parallel plates, thermal entry length solution,  $Pr = 1.0$ , per handbook of heat transfer, 7-101, with Reynolds numbers based on mass fluxes implied by charging analysis. Gas temperature for 0 to 0.5 sec assumed to equal flame temperature.
4. Heat transfer coefficients for 0.5 to 144 sec computed under the assumption of turbulent natural convection. Gas temperatures for 0.5 to 144 sec based on complete mixing of incoming gas and resident gas which loses heat to walls.

Case 2: Nominal gap charging to 0.5 sec, followed by 200 Hz chamber pressure oscillations of 2% amplitude continuing throughout entire duration

Conclusions:

1. For a conservative analysis, 0.125-in. DC 93-104 maintains steel temperatures below 450°F for the duration of the firing (see figure 9-2).
2. It is not believed that the gap, aft of the 0.25-in. insulator, will respond to the chamber pressure oscillations assumed in the analysis and will probably cool in a fashion similar to Case 1.

Assumptions:

1. The gap was assumed to respond to the inflow of flame temperature gas for each cycle so that complete mixing between the incoming

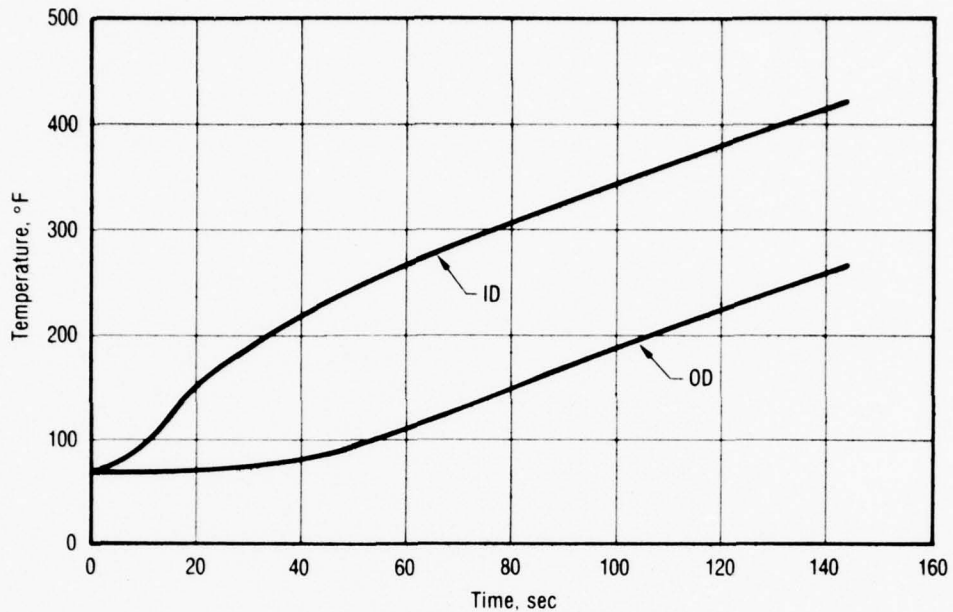


Figure 9-2. Steel Temperature Response - Case 2

(2% Chamber Pressure Oscillation, 200 Hz)

11678

and resident gases takes place; thus, a higher average gap gas temperature is maintained than in Case 1. This is felt to be very conservative, due to the small likelihood of the 85-in. gap responding in such a manner to the high frequency, pulsating flow at the forward end.

2. Heat transfer coefficients and gas temperatures for 0 to 0.5 sec same as Case 1.
3. Heat transfer coefficient for 0.5 to 144 sec computed by pipe flow equation with velocity based on the volume (hence, length) for isentropic compression and one-fourth of the period.

Case 3: Flowthrough condition caused by failure of aft seal

Conclusions:

1. For a conservative analysis, 0.125-in. DC 93-104 maintains steel temperatures below 650°F for duration of firing (see figure 9-3).



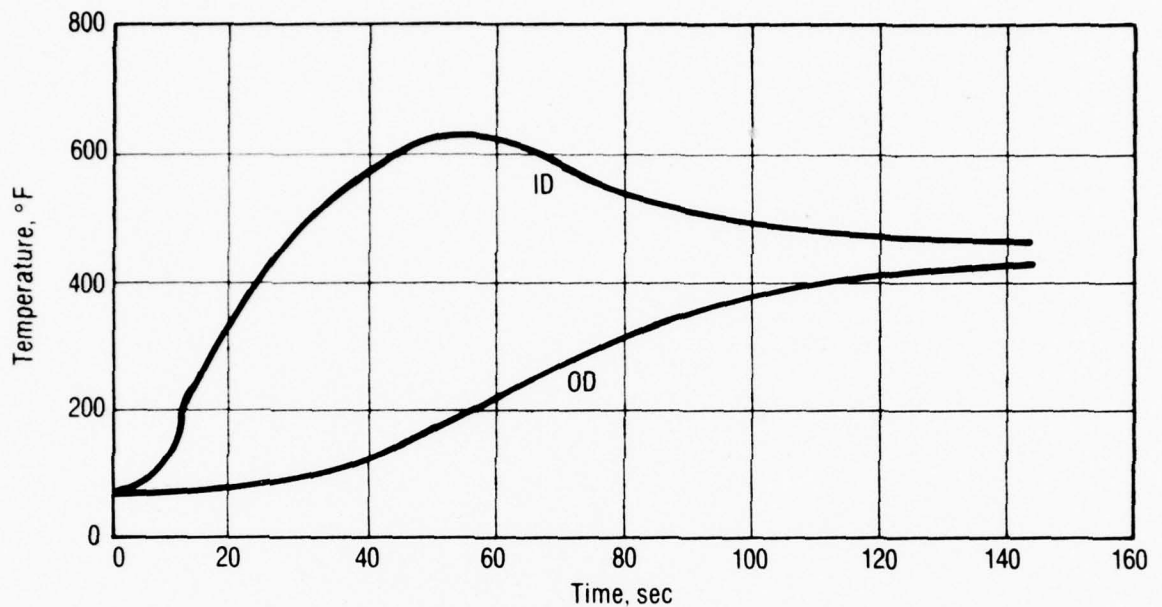


Figure 9-3. Case 3 - Steel Temperature Response  
(Aft Seal Gone/Flowthrough)

11679

2. Analysis is conservative because of failure to account for cooling effect of DC 93-104 pyrolysis gas and mass addition (in gap) pressure loss, which would tend to decrease flow rates.

Assumptions:

1. Gap flow assumed to be driven by the pressure drop down the grain, with aft seal failure at ignition (cartridge to aft insulator seal)
2. Grain pressure drop calculated by:  
 $\Delta P/P = \gamma M^2$ , where M is the aft end Mach number (see figure 9-4).
3. At 50 sec,  $\Delta P$  was so small that for 50 to 144 sec, the Case 1 cooldown phase was assumed.

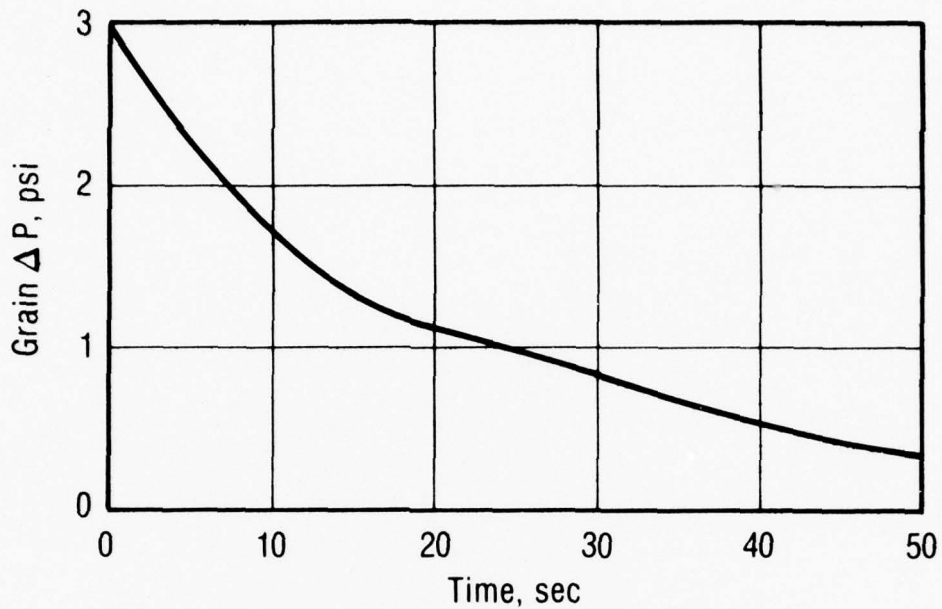


Figure 9-4. Case 3 - SLSH Grain  $\Delta P$  vs Time

11680

4. For 0 to 50 sec, the gap gas flow rates were iterated on until the pressure drop as computed by Fanno line flow matched the grain pressure drop.
5. The above flow rates were used to compute heat transfer coefficients in the manner described for Case 1.
6. The gas temperature for 0 to 50 sec was assumed to equal the flame temperature.

## 10.0 TEST BAY INSULATION

The top of the short length Super HIPPO motor will be 11.4 ft above the pad rails while the concrete wall is 25-ft tall, exclusive of hand railings. To avoid exhaust plume damage to the wall, the motor centerline should be set at least 11 ft from the wall. If thermal wall protection is desired, the DC 93-058 which was used with Super HIPPO/ELSH stand should be considered.

## 11.0 GRAIN MEAN BULK TEMPERATURE

The grain mean bulk temperature should be known if a thorough ballistic analysis is to be made on a firing. The following analysis indicates that, for a grain the size of the Super HIPPO units, the temperature must be monitored and recorded for 30 days before test to get a good measure of bulk temperature. This requires monitoring in the storage area and in the assembled motor.

Two cases were considered in this analysis: (1) nominal conditioning with a mean day temperature of 82°F, and (2) worst case conditioning with a mean day temperature of 99°F. The conditioning period was assumed to be 30 days. Histories of the propellant mean bulk temperatures in both cases are presented in figures 11-1 and 11-2. As shown, 30 days is sufficient time to allow the mean bulk temperature to come within 1°F of the specified mean air temperature in both cases.

The temperatures shown were computed by one-dimensional heat conduction at a typical location on the ELSH case. The internal grain surface was assumed to be adiabatic since the nozzle will be sealed against the environment during the conditioning period. Externally, a convective heat transfer coefficient was computed from the following correlation of average heat transfer coefficient for a circular cylinder in cross flow with air:

$$\text{Nu} = 0.0239 \text{ Re}^{0.805}$$

A time dependence was introduced by using WTR mean hourly weather data to compute the Reynolds number. Air temperatures were computed assuming a sinusoidal variation of 20°F about the specified mean temperatures with a period of 1 day. Minimum and maximum air temperatures were assumed to occur at 3 a.m. and 3 p.m.

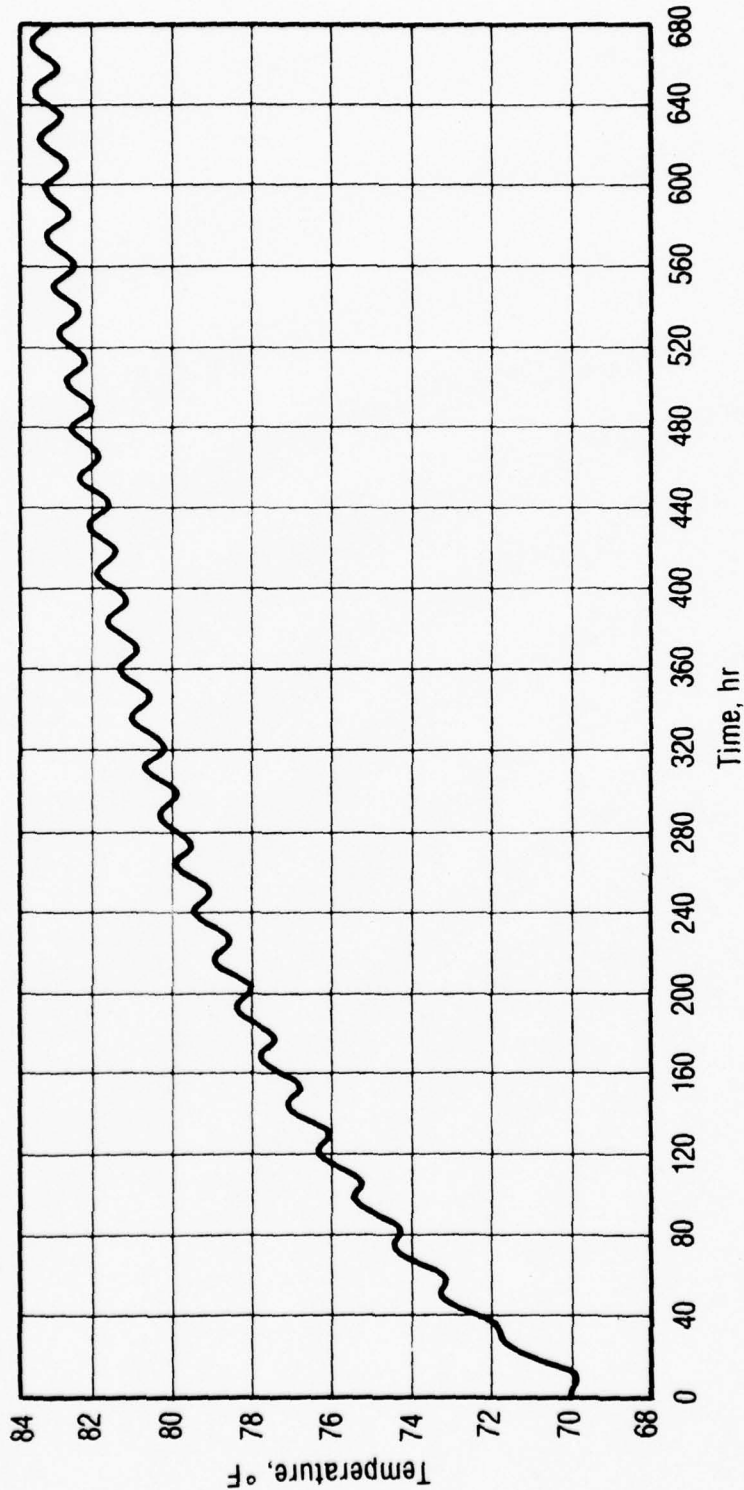


Figure 11-1. Propellant Grain Mean Bulk Temperature vs Time for 70° Grain Exposed to 82° Mean Daily Temperature

11663

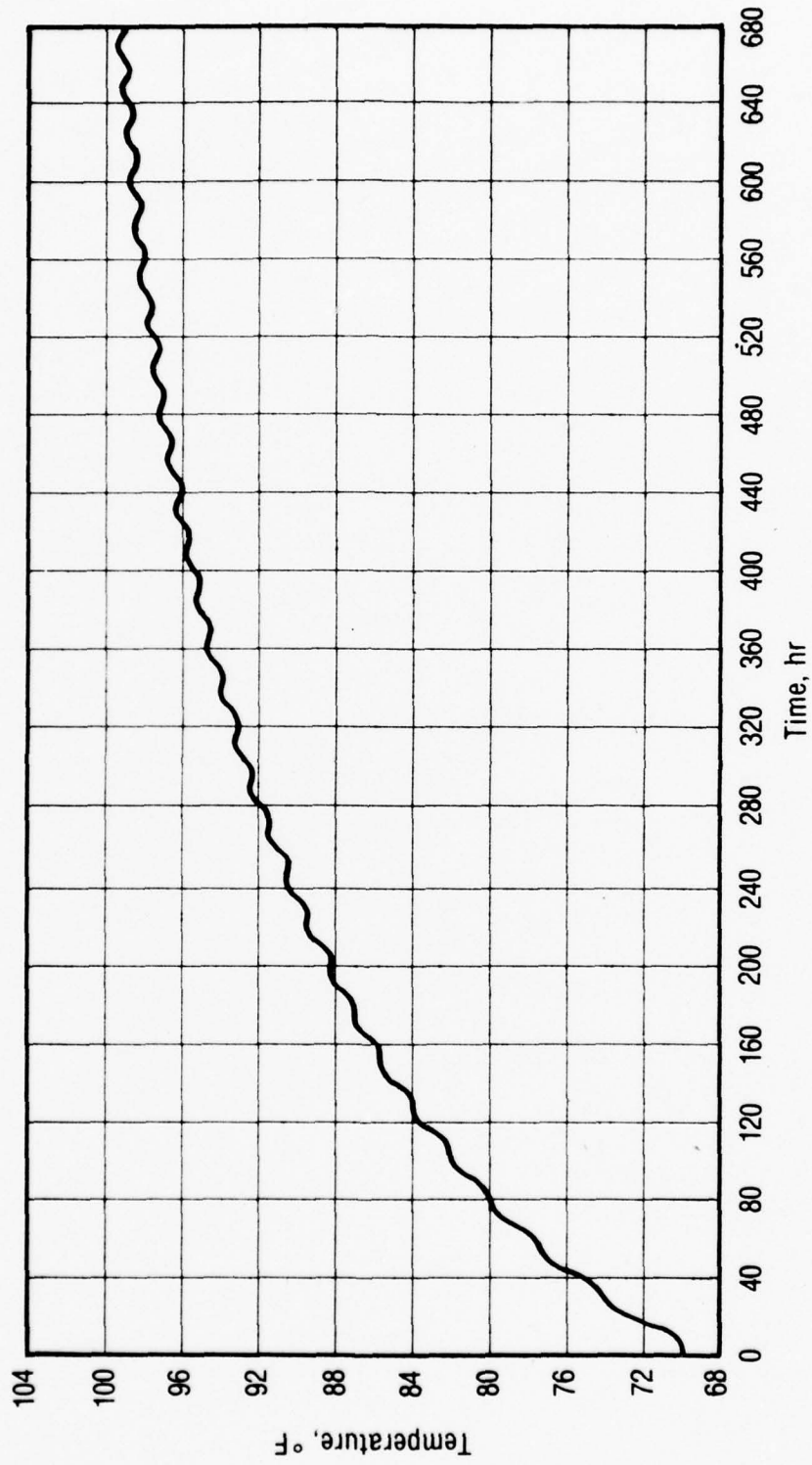


Figure 11-2: Propellant Grain Mean Bulk Temperature vs Time for 70° Grain Exposed to 99° Mean Daily Temperature

11664

## 12.0 PHILOSOPHY OF RECYCLE OF INSULATION

The following plan is based upon the thermal analysis performed to predict insulation requirements for five firings similar to the demonstration firing (40 sec at 1,500 psi). Actual service life may vary as different propellants and duty cycles may be experienced. The components are discussed below starting at the nozzle and working forward.

### 12.1 ADAPTER INSULATOR

This item is considered as a portion of the nozzle. A new adapter insulator should be designed and fabricated for each nozzle to be tested. This is not in the scope of contract No. F04611-77-C-0027.

### 12.2 AFT CLOSURE

The aft closure insulator is rated at five tests. One insulator and two sets of plugs (to protect the retaining screws) will be provided. The capability for 145-sec duration tests at 800 psi is two tests. Since the cost of fabricating this part is quite high, even badly eroded insulators should not be discarded without project review to consider rework techniques.

The rectangular strip of rubber around the inside face of the aft insulator is bonded with EPON 913. This item should be replaced after each test.

### 12.3 CARTRIDGE

The cartridge requires some refurbishment as a normal part of the reloading cycle. The forward restrictor of the aft closure is consumed on each firing. The rubber insulation inside the wall can be ground clean, patched locally with potting compound, and patched over larger areas with sheets of cured rubber. Eroded parts of the fiberglass surface can be built up with an epoxy-milled glass mixture. Sealing surfaces can be cleaned with surfacing resin. This refurbishment is a portion of routine reloading activities.

#### 12.4 CARTRIDGE SPACER

The cartridge spacer also requires periodic refurbishment. Since the spacer is returned with the cartridge on the shipping pallet, this refurbishment is included in the reloading contract.

#### 12.5 FORWARD INSULATOR

The forward insulator consists of a large asbestos-phenolic disc which is expected to last 10 firings and smaller rubber discs which are replaceable after each test. The rubber discs are readily removable from the phenolic part, and are replaceable with two-face tape. Estimates of service life or thickness required for the rubber disc depend on the pressure, duration, and temperature of a test. The char rate is approximately 1/2 in./min at 1,000 psi. The diameter of the rubber was made large enough to protect the phenolic portion for extended service life. The rubber erodes deeply at the center and negligibly at the outer diameter.

Radial strips of rubber 3/4 by 1 by 6 in. are placed on the forward insulator to keep the forward restricter from sagging onto the forward insulator. Additional strips are used for low-modulus propellant. Those are replaced each time.

#### 12.6 CASE WALL INSULATION

A 1/4-in.-thick rubber insulator is bonded to the case wall to protect the steel locally where combustion gases enter the gap external to the cartridges. A spare rubber insulator will be provided. Replacement is by removal and rebonding new units.

Above the bonded-in rubber insulation, DC 93-104, a room curing silicone-base insulation rubber is installed. The short length motor insulation thickness is increased from 0.03 to 0.125 in. to accommodate the long durations. Refurbishment is by burnishing the rubber surface and applying additional coats of insulation.



## 13.0 HANDLING OF SLSH MOTOR COMPONENTS

### 13.1 FORWARD CLOSURE (WEIGHT ~18,000 LB)

The forward closure (C10119) has two trunnions (C10289) permanently attached. The centerline formed by these two trunnions is 5-1/2 in. offset from the center of gravity of the closure so that a third lift point is required. A 1-1/2-6 eyebolt provides the third point. The trunnions each have two journal sections: 2-in.-wide journals inboard for lifting hooks or stirrups and 6-in.-wide journals outboard for support in the trunnion base. The closure is lifted by use of the C10292 sling assembly using C11151 stirrups to attach to the 2-in. trunnion journals. A tag leg on the sling attaches to eyebolt.

The closure can be placed in the C10291 trunnion base using the C10849 support under the overbalance side. The stirrups become captive on the trunnions and must be disconnected from the C10292 sling. The closure can be inverted by attaching a crane hook to the 1-1/2 in. eyebolt and swinging it over the top. The crane must be capable of translation to keep the lift cable vertical so as to avoid putting horizontal loads into the trunnions.

The C10713 transport trailer has similar trunnion base supports and can be used for working on, inverting, and transporting of closures. The C10713 drawing contains instructions for positioning the support heads to level the closure.

The forward insulator is moved using the C10300 and three 1/2-13 eyebolts screwed into the threaded holes. The rubber portion of the forward insulator is moved manually.

### 13.2 CASE (WEIGHT ~13,000 LB)

The case is lifted by attaching a C10290 case lift adapter with four each of the C10840 pins. The C10290 adapter has journals identical to the C10289 trunnions. The case is lifted using the C10292 sling and the C11151 stirrups connected to the 2-in.-wide journals. The case should never be set on the concrete, but always on plywood or wood blocks to avoid scratching.

If the case is to be inverted, it is lowered onto another C10290 adapter and attached so that the adapters are parallel. The assembly is then lowered so that the wide journals of the lower case lift adapter engage the C10291 trunnion base. The case can then be lowered into a wooden cradle for storage or refurbishment. Care must always be taken to avoid scratching the O-ring surfaces inside the motor case. The lift adapters should be removed for any extended storage to avoid rust of the case. When lowering the case on to the closure, always use the 20,000-lb hydroset for smooth controlled engagement.

### 13.3 AFT CLOSURE (WEIGHT ~19,000 LB)

The aft closure has C10289 trunnions permanently attached exactly as the forward closure. It is handled in the same manner with the same fixtures. The aft closure is conveniently processed on the C10713 transport trailer. This allows the nozzle and closure subassembly to be put together inside a remote building to control sand, dust, and temperature. The preferred assembly sequence is to invert the closure for installation of the aft closure insulator, O-rings and retainers, then to rotate the closure upright for installation of the insulated nozzle adapter and/or nozzle. The nozzle/closure assembly can then be placed on the case as an assembly (using the hydroset).

### 13.4 PROPELLANT CARTRIDGE (WEIGHT TO 28,000 LB)

The propellant cartridges are shipped and stored on PD2492 shipping bases. The C10714 transport trailers will transport either CHAR or Super HIPPO grains on their respective bases. The propellant cartridges are lifted, loaded into motors, and removed from motors using the C10294 cartridge lift adapter. The lift adapter must be adjusted so the four lift points are locked, and engage the fiberglass by  $1\frac{1}{8}$  in. The four safety latches must be engaged over the cartridge and pinned while lifting the propellant cartridge except for the final 2 ft of vertical travel while loading/unloading the cartridges in the motor case (see appendix E).

### 13.5 MISCELLANEOUS

The handling equipment also includes C10741 and C10742 spanners for installing of insulation plugs, PD2493 clevis pin shipping containers, and a C11029 hydroplug for the C10120 aft closure during hydrotest.

The C11198 shear key test fixture can be used to qualify new shear key samples.

APPENDIX A  
THRUST STAND STRESS ANALYSIS

Reference drawing C12418, AISC code

AXIAL LOADS

Thrust Load = 10,000,000 x 2 = 20,000,000 (FS = 2)

Compr. Area = 4 (6)(2)(14) + (3)(2)(10) = 912 in.<sup>2</sup>

$f_a = 20,000/912 = 21.93$  ksi compr.

$b/t = 14/2 = 7 < 76/(f_y)^{1/2} = 12.6$

$r = (0.29)t = 0.29(2) = 0.58$

$1/r = 18/.58 = 31$  ;  $F_a = 19.87$  ksi

t = 2 in.

Minimum FS = 1.67 giving a buckling stress = (1.67)(19.87) = 33.18 ksi

$$MS = \frac{33.18}{21.93} - 1 = +0.51$$

Welded box sections would provide a larger FS.

SIDE LOADS

Side thrust load = 81,000 at height = 217 in. with Super HIPPO motor  
vertical load = 300,000 lb ; Motor weight = 55,000 lb

Allenoy steel bolts;  $F_y = 153$  ksi ;  $F_{tu} = 170$  ksi

Overturning moment = (81)(217) = 17,577 k in. (2 @ 1 in. bolts at 68 in.)

Bolt load = (17,577k/(2)(68) - (355k/8) = 129k - 44k = 84,600/bolt

$f_t = 84.6/0.606 = 139.6$  ksi tensile

$f_v = 81 / [(4)(.7854) + (4)(1.2273)] = 10.1$  ksi (4 at 1 in. and 4 at 1-1/4 in.)  
(threads excluded)

Yield Interaction:

$$\left( \frac{10.1}{(0.577)(153)} \right)^3 + \left( \frac{139.6}{153} \right)^2 = 0.0015 + 0.8325 = 0.834$$

$$\text{Yield MS} = \frac{1}{\sqrt{0.834}} - 1 = +0.09$$

Note: Prying action not included as details are not available.  
For short length motors, loads are about half of above values.

APPENDIX B  
SUPER HIPPO DRAWING LIST

<u>SIZE</u>	<u>DWG.</u>	<u>CH.</u>	<u>ECO</u>	<u>TITLE</u>
E-3	C10118	C		Case, Motor - Super HIPPO
E-2	C10119	F	20505	Closure, Fwd - Super HIPPO
E-2	C10120	F		Closure, Aft - Super HIPPO
Q-1	C10121	N/C		Pin, Locating - Super HIPPO
C-1	C10141	N/C		Pin, Straight - Super HIPPO
E-1	C10142	N/C		O-ring Retainer - Super HIPPO
Q-1	C10144	C	20492	O-ring Packing - Super HIPPO
C-1	C10276	N/C		Plug, Insulation, Aft - Super HIPPO
Q-1	C10277	C		Insulator, Fwd - Super HIPPO
Q-1	C10278	C		Spacer, Cartridge - Super HIPPO
E-1	C10279	D		Cartridge, Insulated - Super HIPPO
E-1	C10280	B	20374	Insulation, Outer-Aft Closure - Super HIPPO
E-1	C10283	B		Key, Lock, Adapter - Super HIPPO
J-1	C10286	B		Motor Assembly Hydrostatic Test Configuration - Super HIPPO
E-1	C10289	C		Trunnion Shaft - Super HIPPO
E-1	C10290	A		Adapter, Lifting - Case - Super HIPPO
E-1	C10291	N/C		Trunnion Base
E-1	C10292	N/C		Sling
C-1	C10293	A		Plug
E-2	C10294	B		Cartridge Lift

<u>SIZE</u>	<u>DWG.</u>	<u>CH.</u>	<u>ECO</u>	<u>TITLE</u>
E-2	C10295	C		Loaded Cartridge
E-1	C10297	A		Plug Nozzle Shell
E-1	C10299	A		Nozzle Assembly 12.5" Sub
E-2	C10300	A		Nozzle Lift
E-1	C10712	N/C		Transport, Trailer, Modification Stage I - Super HIPPO
E-1	C10713	N/C		Transport Trailer, Closure - Super HIPPO
E-1	C10714	N/C		Transport Trailer, Cartridge - Super HIPPO
E-1	C10715	A		Transport Trailer, Handling Equipment - Super HIPPO
C-1	C10741	N/C		Wrench, Spanner - Small Insulation Plug, Super HIPPO
C-1	C10742	N/C		Wrench, Spanner - Large Insulation Plug, Super HIPPO
E-1	C10761	N/C		Fixture, Leak Test - Super HIPPO
Q-1	C10762	N/C		Plug, Leak Test - Super HIPPO
C-1	C10840	N/C		Pin Assembly
E-1	C10849	N/C		Support Trunnion
D-1	C00631	C		Igniter
	PD2492	B		Cartridge Pallet
	PD2493			Pin Box
D-1	C11007	C		Extended Super HIPPO Case Joint Ring
E-1	C11012	N/C	20461	Insulator Aft
E-1	C11014	A		Adapter
E-1	C11015	A		Backup Key

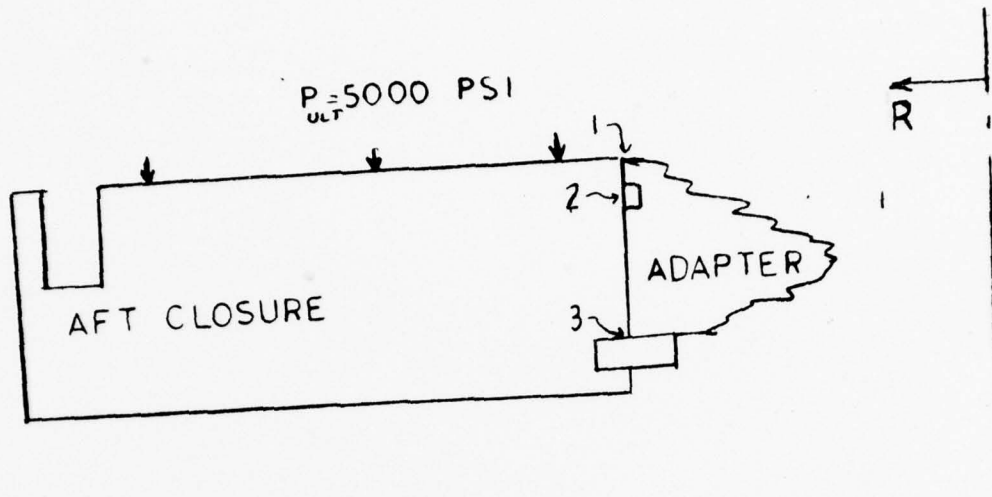


<u>SIZE</u>	<u>DWG.</u>	<u>CH.</u>	<u>ECO</u>	<u>TITLE</u>
D-1	C11021	C		Insulation, Joint Ring
E-3	C11125	B		Aft Case
E-2	C11126	D		Closure
E-1	C11029	N/C		Plug, Aft Closure
J-1	C11142	A		Nozzle Assembly
D-1	C11151	A		Stirrup, Lifting
J-1	C11167	D	20496	Motor Assembly
E-1	C11198	A		Test Fixture, Lock Key
D-1	C11199	N/C		Segmented, Ring, Centering
E-1	C11301	N/C		Lock Key, Test, Segmented
J-2	C11347	G	20378	Motor Assembly, Super HIPPO, Extended
D-1	C11369	N/C		Insulation, Restrictor
J-1	C11374	C		Hydrostatic Test Assembly, Super HIPPO, Extended
D-1	C11478	N/C		Restrictor, Aft
E-2	C11479	A	20159, 20377	Loaded Cartridge - Length - Super HIPPO
C-1	C12028	N/C		Clip, Retention, Shear Key
E-1	C12037	N/C		Shear Key - ELSH
	C12419	N/C		Case, Short Length
	C12418	N/C		Support, Case
	C12416	N/C		Cover Hydro (Char)
	C12420	N/C		Hydro Assembly - SLSH/IUS
	C12411	N/C		Assembly - SLSH/IUS
	C12590			Insulation Ring, Nozzle Adapter
	C12592			Ring Nozzle Adapter

<u>SIZE</u>	<u>DWG.</u>	<u>CH.</u>	<u>ECO</u>	<u>TITLE</u>
	C12716			Cartridge Insulated
	C12629			Cartridge, Loaded, IUS
	C12413	N/C		Loaded Assembly - SLSH
	C12417	N/C		Hydro Assembly - SLSH

APPENDIX C  
STRESS ANALYSIS RESULTS

RELATIVE MOTIONS IN O RING SEAL AREAS BETWEEN AFT CLOSURE AND ADAPTER .



POINT	$\Delta R$ CLOSURE	$\Delta R$ ADAPTER
1	-0.078	
2	-0.060	
3	0.066	

## SUPER HIPPO JOINT ANALYSIS

THE CASE AND CLOSURES ROTATE IN OPPOSITE DIRECTIONS. A UNIT ANALYSIS WAS MADE ON BOTH TO DETERMINE THE ROTATION VS. MOMENT RELATIONSHIP AS SHOWN BY FIGURE B. THE INTERSECTION OF THE TWO CURVES IS THE MOMENT THE JOINT SHOULD SEE. A MOMENT OF 65,000 IN-LB/IN WAS DETERMINED. THE AFT CLOSURE GAVE LESS ROTATION.

Rotation of case and closure at clevis pins  
vs. moment transmitted through clevis pins

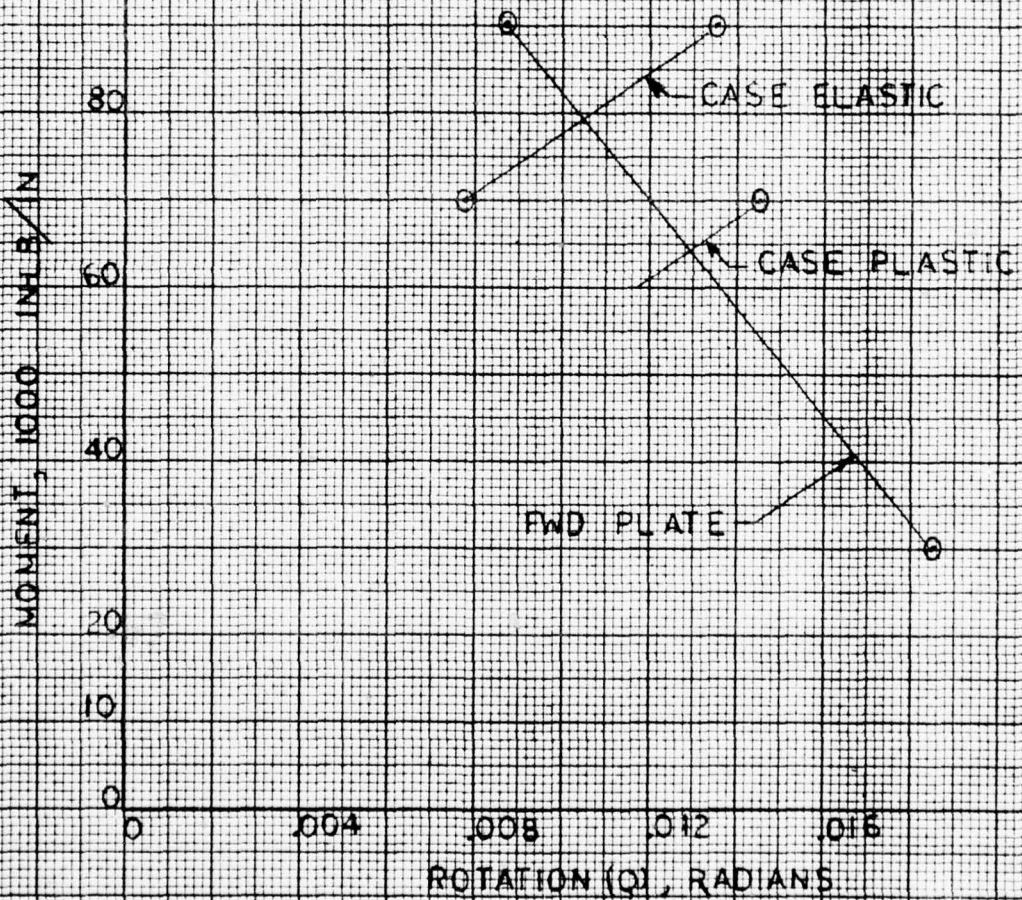
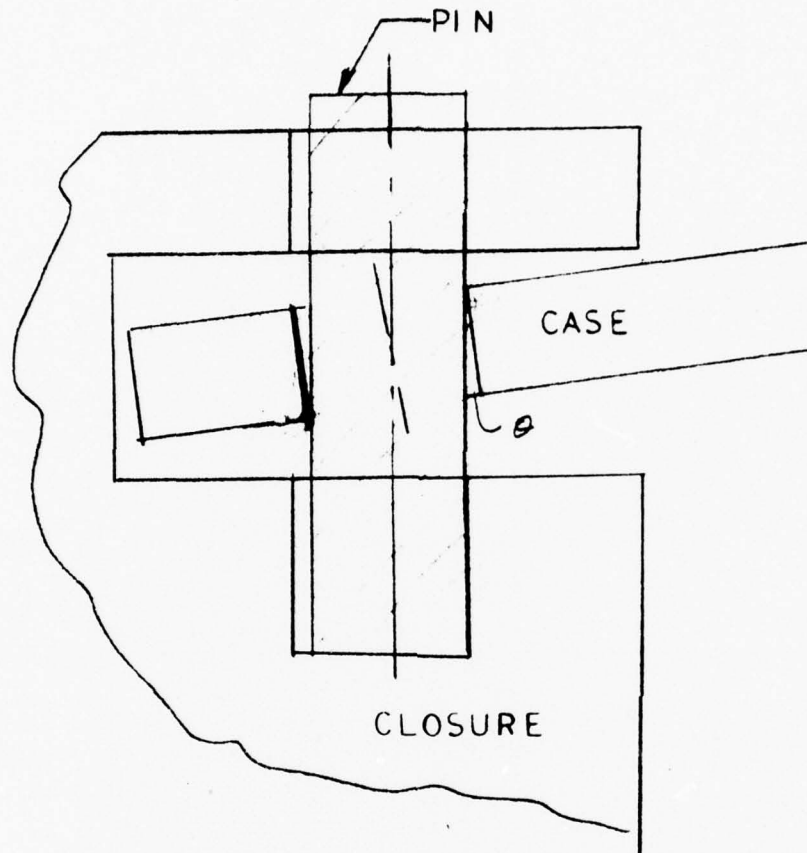


Figure B  
66

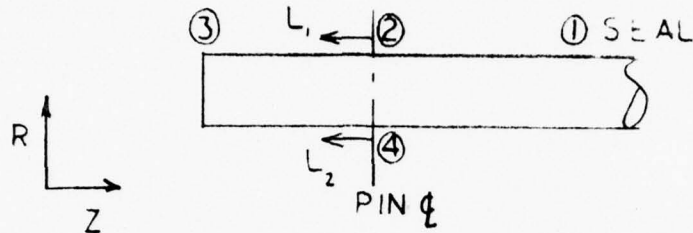


CASE PIN DIA = 2.261 MIN  
 PIN DIA = 2.250 MAX

$\theta = 0.011 / 1.7 = 0.065$  RAD ROTATION OF  
 CASE RELATIVE TO CLOSURE DUE TO  
 CLEARANCE IN PIN HOLES.  
 ADD. ROTATION DUE TO BEARING  
 DEFORMATION WILL ALSO REDUCE  
 MOMENT ON CASE

JOINT ANALYSIS CASE

TWO ELASTIC AND ONE PLASTIC FE RUNS WERE MADE ON THE CASE.



RUN # 1

$L_1 = 0$   
 $L_2 = 2.78 \times 10^7 \text{ LB}$   
 $M = 89,600 \text{ IN-LB/IN}$   
 $\theta = .0134 / 1.7 = .0079 \text{ RAD}$

	1	2	3	4
$\Delta R$	.066	.0745	.103	.076
$\Delta Z$	-.0456	-.0385	-.037	-.06094

RUN # 2

$L_1 = 3.1 \times 10^6 \text{ LB}$   
 $L_2 = 2.47 \times 10^7 \text{ LB}$   
 $M = 70,000 \text{ IN-LB/IN}$

	1	2	3	4
$\Delta R$	.068	.063	.078	.064
$\Delta Z$ ELASTIC	-.047	-.0429	-.041	-.0557
$\Delta Z$ PLASTIC		-.0425		-.0577

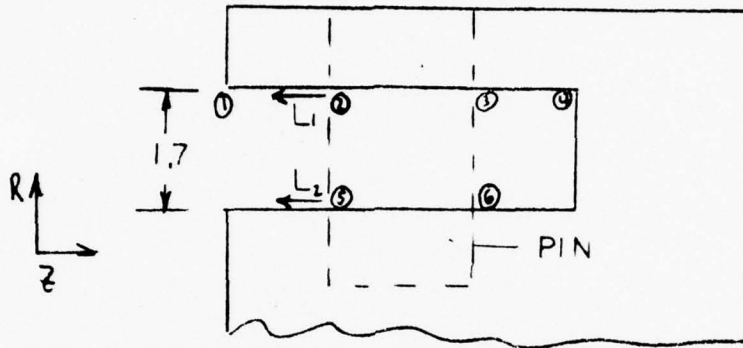
$\theta_E = .0134 / 1.7 = .0079 \text{ RAD}$

$\theta_P = .0152 / 1.7 = .009 \text{ RAD}$



## JOINT ANALYSIS FWD CLOSURE

TWO FE RUNS WERE MADE TO DETERMINE  
ROTATION OF FWD CLOSURE JOINT DUE TO  
MOMENT AT PINS



RUN #1

$$L_1 = 9.3 \times 10^6 \text{ LB}$$

$$L_2 = 1.85 \times 10^7 \text{ LB}$$

$$M = \frac{4.6 \times 10^6 \times 1.7 \text{ IN}}{2 \times \pi \times 42} = 29,600 \text{ IN-LB/IN}$$

$$\theta = .0315 / 1.7 \text{ RAD.}$$

	1	2	3	4	5	6
$\Delta R$	-0.031	-0.0170	0	+0.0148	-0.032	-0.003
$\Delta Z$	-4.40	-4.402	-4.355	-4.321	-4.070	-4.057

RUN #2

$$L_1 = 0$$

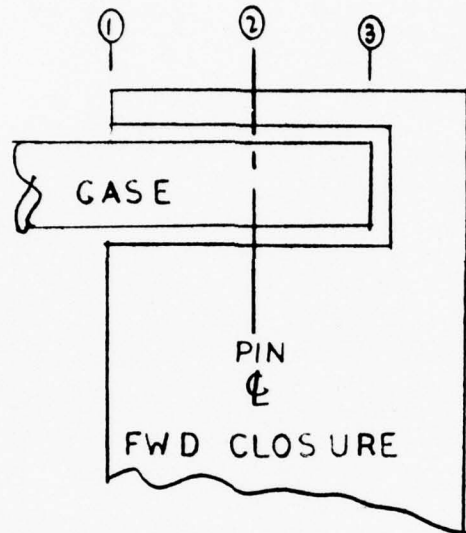
$$L_2 = 2.78 \times 10^7 \text{ LB}$$

$$M = \frac{1.39 \times 10^7 \times 1.7}{2 \pi \times 42} = 89,600 \text{ IN-LB/IN}$$

$$\theta = .015 / 1.7 \text{ RAD.}$$

	1	2	3	4	5	6
$\Delta R$	-0.045	-0.0219	0	+0.0158	-0.031	-0.002
$\Delta Z$	-4.13	-4.122	-4.116	-4.109	-3.934	-3.910

## JOINT DEFLECTIONS



THE JOINT HAS A 0.1 IN CLEANCE BETWEEN  
CASE OD AND PLATE FLANGE UNPRESSURIZED

	1	2	3
FLANGE $\Delta R$	-0.043	-0.022	+0.015
CASE $\Delta R$ ELASTIC	.067	.069	.090
CASE $\Delta R$ PLASTIC	.062	.063	.082

## SUPER HIPPO PINS

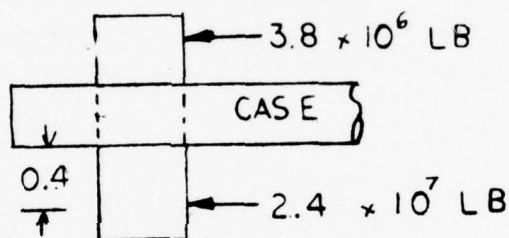
MATERIAL 4340 STEEL

$$F_{TU} = 180,000 \text{ PSI}$$

$$F_{SU} = 109,000 \text{ PSI}$$

### AXIAL LOAD

FROM JOINT ANALYSIS



$$\text{LOAD/PIN} = 2.4 \times 10^7 / 60 = 400,000 \text{ LB/PIN}$$

$$\text{SHEAR AREA} = \frac{\pi}{4} D^2 = \frac{\pi}{4} 2.25^2 = 3.98 \text{ IN}^2$$

$$\tau = 400000 / 3.98 = 100000 \text{ PSI}$$

$$MS = \frac{109000}{100000} - 1 = \underline{\underline{+0.09}}$$

### MOMENT

$$M = 400000 \times 0.4 = 164000 \text{ IN/LB}$$

$$I = 1.258$$

$$\sigma = \frac{164000 \times 1.2}{1.258} = 142000 \text{ PSI}$$

$$MS = \frac{180000 \times 1.6}{142000} - 1 = +1.0$$

SUPER HIPPO - AFT CLOSURE (C10120)

MATERIAL 4340 NORMALIZED & TEMP.

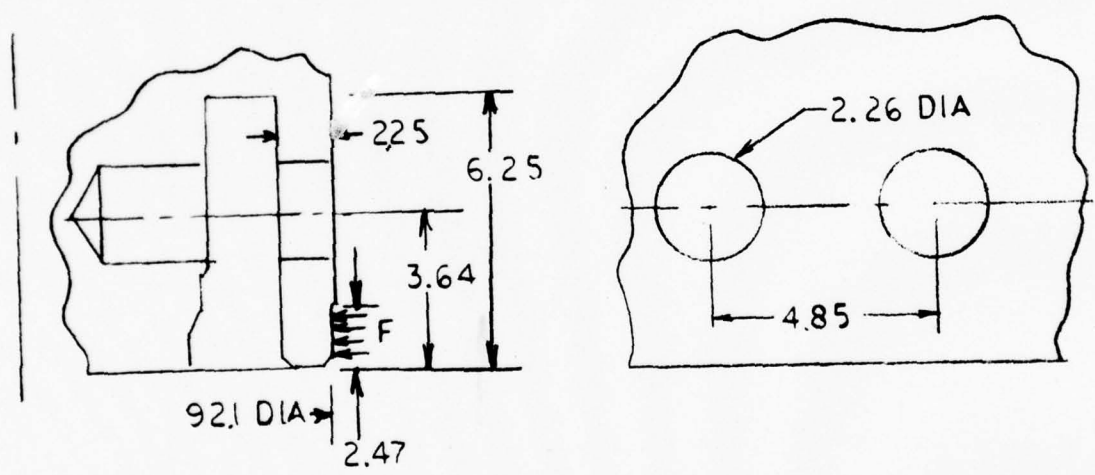
$$F_{TU} = 125000 \text{ PSI}$$

HOOP STRESS F.E. ANALYSIS MADE WHICH GAVE  
A MAX STRESS AT THE INSIDE EDGE OF:

$$\sigma_H = 105000 \text{ PSI}$$

$$MS = \frac{125000}{105000} - 1 = +0.19$$

BENDING DUE TO SIDE LOAD



$$F = 80000 \times 2(SF) = 160000 \text{ LB SIDE LOAD APPLIED BY TEST STAND RING}$$

$$\text{LINE LOAD} = \frac{F}{R} = \frac{160000}{46} = 3500 \text{ LB/IN}$$

AT PIN Q

$$M = 3500 \times (3.64 - 1.2) = 8500 \text{ IN LB}$$

$$\sigma = \frac{6M}{T^2} = \frac{(6)(8500)}{2.25^2} \times \frac{4.85}{4.85 - 2.26} = 19000 \text{ PSI}$$

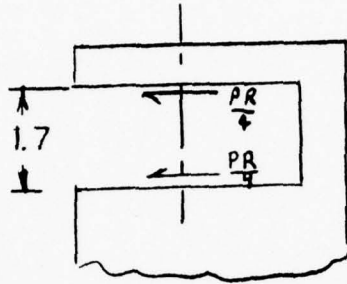
$$\frac{1}{2} \times \frac{PR}{2T} \times \frac{4.85}{2.59} = \frac{5000 \times 46 \times 4.85}{2 \times 2 \times 2.59 \times 2.25} = 48000$$

$$MS = \frac{125000}{48000 + 19000} - 1 = +0.86$$

AFT CLOSURE (CONT.)

BENDING DUE TO PIN LOAD

WORST CASE ASSUME 1/2 OF LOAD IN OUTSIDE FLANGE. JOINT ANAL. SHOW IT WAS LESS.



$$\text{LOAD} = PR/4 \approx 52500 \text{ LB/IN}$$

$$\text{MOMENT } 52500 \times 1.7 = 89000 \text{ IN-LB/IN}$$

$$\sigma = \frac{6M}{T^2} = \frac{6 \times 89000}{3.75^2} = 38000 \text{ PSI}$$

$$MS = \frac{125000}{38000} - 1 = \underline{\underline{+2.3}}$$

SUPER HIPPO FWD CLOSURE (C10119)

MATERIAL: 4340 STEEL PER MIL-S-5000 COND. E

$$F_{TU} = 125000 \text{ PSI}$$

LOAD

$$P_{ULT} = 5000 \text{ PSI}$$

STRESS

TREATED AS SIMPLY SUPPORTED PLATE  
ROAK P.194 CASE 1

$$S_{MAX} = \frac{3 P \pi R^2 (3M+1)}{8 \pi M T^2}$$
$$= \frac{3 \times 5000 \times 42.1^2 \times 11}{8 \times 33 \times 10^2} = 113000 \text{ PSI}$$

$$MS = \frac{125000}{113000} - 1 = +\underline{\underline{0.1}}$$

FINITE ELEMENT ANALYSIS GAVE A MAX STRESS  
OF:

$$\sigma_{HOOP} = 115000 \text{ PSI}$$

$$MS = \frac{125000}{115000} - 1 = +\underline{\underline{0.08}}$$

SUPPER HIPPO CASE (C12419)

MATERIAL HY-130 PER MIL-S-24371

$$F_{TU} = 140,000 \text{ PSI}$$

$$F_{TY} = 130,000 \text{ PSI}$$

$$F_{SU} = \frac{5}{8} F_{TU} = 87,600 \text{ PSI}$$

LOAD

$$P_{ULT} = 5000 \text{ PSI}$$

HOOP STRESS

$$\sigma = PR/T = 5000 \times 42 / 1.57 = 134,000 \text{ PSI}$$

$$MS = \frac{140000}{134000} - 1 = +0.04$$

EDGE TEAR OUT

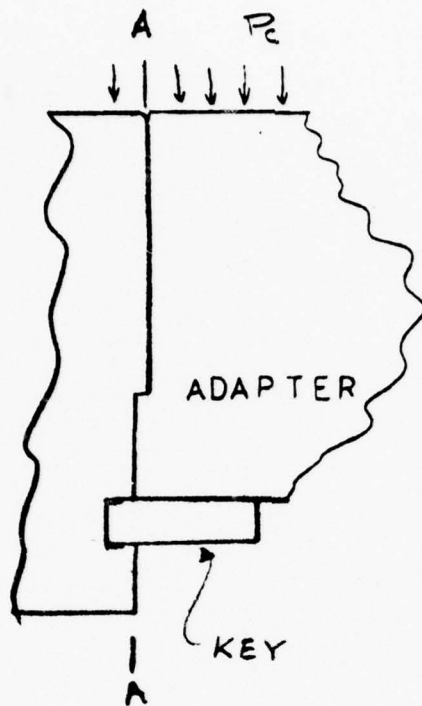
$$\text{LOAD/PIN} = P\pi R^2/60 = 464,000 \text{ LB}$$

$$\begin{aligned} \text{SHEAR AREA} &= 2 \text{ SIDES} \times (2.55 - 1.13) / .707 \times 1.6 \\ &= 6.5 \text{ IN}^2 \end{aligned}$$

$$\tau = 464000 / 6.5 = 71400 \text{ PSI}$$

$$MS = \frac{87600}{71400} - 1 = \underline{\underline{+0.2}}$$

KEY



SECTION A

$$\text{LOAD} = PR/2 \quad 21.23 \times 5000 / 2 = 53000 \text{ LB/IN}$$

SHEAR

$$\tau = 53000 / 1 = 53000 \text{ PSI}$$

$$MS = \frac{109000}{53000} - 1 = +1.0$$

BEARING

$$\tau_b = 53000 / 45 = 118000 \text{ PSI}$$

$$MS = \frac{250000}{118000} - 1 = +1.0$$

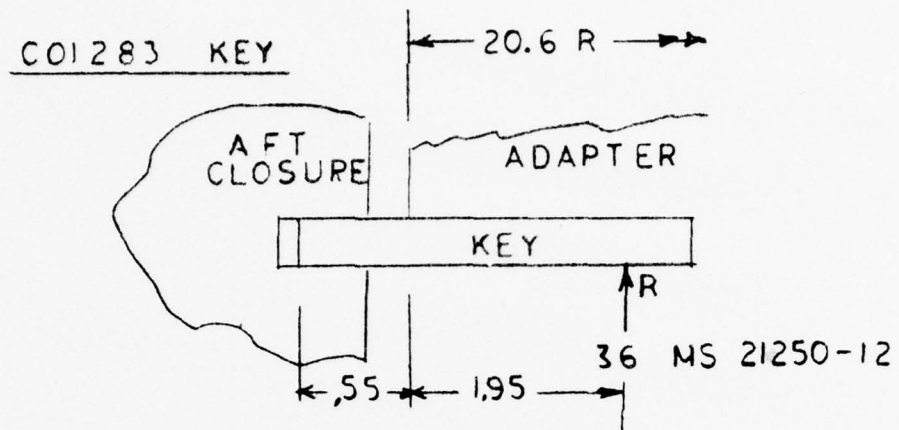
BENDING

$$\sigma = 6M/T^2 = 6 \times 45 \times 53000 / 1 = 143000 \text{ PSI}$$

$$MS = \frac{180000}{143000} - 1 = 0.2$$



ADAPTER KEY BOLTS



$$\text{LOAD} = P \uparrow R^2 / 36 = 185000 \text{ LB} / \text{BOLT}$$

ASSUME LOAD CENTER .2 FROM EDGE

$$\sum M = 0$$

$$.55 \times 185000 = R \times 1.75$$

$$R = 58,000 \text{ LB}$$

$$R_{\text{ALL}} = A \times F_{\text{TU}} = 0.366 \times 180,000 = 66,000 \text{ LB}$$

$$\text{MS} = \frac{66 \text{ K}}{58 \text{ K}} - 1 = +0.1$$

APPENDIX D

SHEAR KEY SECTOR TESTS

APPENDIX D  
SHEAR KEY SECTOR TESTS

The notched shear key for the Super HIPPO motor must be designed to fail at a carefully controlled chamber pressure to protect the motor case from overpressure. When the prescribed pressure is reached, the shear key fails and allows the nozzle to blow out of the aft closure to vent the gases. To accomplish this accurately, the force required to shear a unit length of notched metal must be controlled. A test fixture was designed to shear two short notched sectors at a time with a maximum force of less than 300,000 lb, the capacity of the available load test machine. Two shear key rings were then made from a single plate of 4340 steel and heat treated in a single furnace charge. One ring was cut into 45 sectors per CSD drawing C11301 for testing in the fixture; the other was machined into the deliverable shear key per drawing C10283 with notch depth determined from test results. Rockwell C hardness of the sectors was 32/34 instead of 26/28. This discrepancy was accepted because the test sectors and deliverable ring were of the same hardness.

Figures D-1 through D-4 show the fixture partially assembled, fully assembled, and mounted in the Tinius Olsen load test machine.

Test sectors were prepared so that the thickness of the material remaining after notching was .3, .4, and .5 in. Five pairs of sectors were prepared for each of these thicknesses. Table D-1 shows test results of rupturing the samples. Figure D-5 is a typical load-force diagram from the machine. Figure D-6 shows typical test sectors before and after rupture. Based on these results, sectors with a thickness of material remaining between notches of .35 in. were made and tested. Half of these later sector pairs were tested as earlier with time to failure of about 50 sec, and half were tested at maximum crosshead speed, about 2 sec to failure. Indicated failure loads reduced about 15 percent at the higher rate.

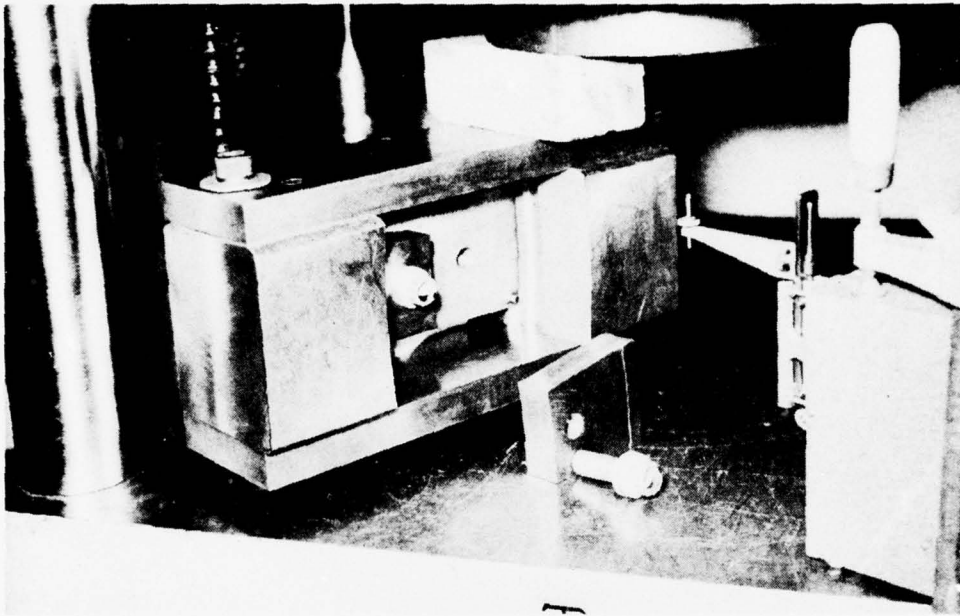


Figure D-1. Shear Key Test Fixture, View 1

9361-1

11181

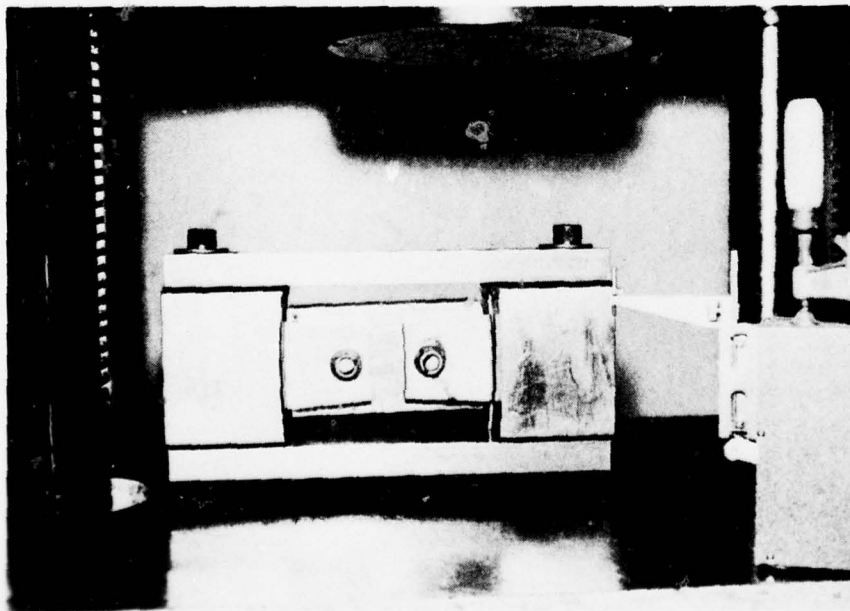


Figure D-2. Shear Key Test Fixture, View 2

9361-2

11182



Figure D-3. Shear Key Test Fixture, View 3

9361-3

11183

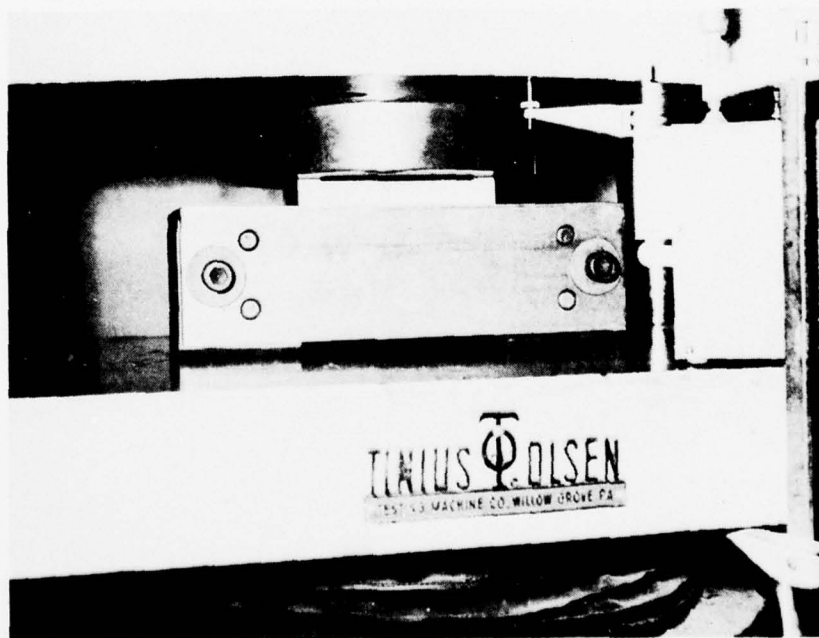


Figure D-4. Shear Key Test Fixture, View 4

9361-4

11184

TABLE D-1. TEST RESULTS OF RUPTERING THE SAMPLES

T1872

Test no.	T, Thickness, (in.)	F, Maximum load at failure	F/Width, failure load lb/in. (F/5.565)	F/Width, group average	Sample no.	Angle notch to rolling direction, (degrees)
1	.4	163,250	29,335	29,129	4 and 26	32
2	.4	165,000	29,649		12 and 34	84
3	.4	161,250	28,975		8 and 30	64
4	.4	162,000	29,110		20 and 42	20
5	.4	159,000	28,571		16 and 38	56
6	.5	196,500	35,309	35,606	3 and 25	24
7	.5	194,500	34,950		11 and 33	88
8	.5	201,000	36,118		7 and 29	56
9	.5	202,500	36,388		19 and 41	28
10	.5	196,250	35,265		15 and 37	60
11	.3	104,750	18,823	19,478	1 and 23	0
12	.3	104,750	18,823		5 and 27	40
13	.3	113,250	20,350		9 and 31	72
14	.3	113,000	20,305		13 and 35	76
15	.3	106,250	19,092		17 and 39	44
16	.3	90,050 <sup>a</sup>	16,181	16,181	21 and 43	12
17	.3					
18						
19		Rebreak tests				
20		results very low				
21		or improperly high				
22		due to joining				
23						
24	.35	112,000	20,125	20,993	2 and 24	16
25	.35	125,500	22,461		10 and 32	80
26	.35	113,500	20,395		6 and 28	48
27	.35	99,000 <sup>a</sup>	17,789	17,729	18 and 40	36
28	.35	99,250 <sup>a</sup>	17,834		14 and 36	68
29	.35	97,750 <sup>a</sup>	17,565		22 and 44	16
30						

<sup>a</sup> High load rate test

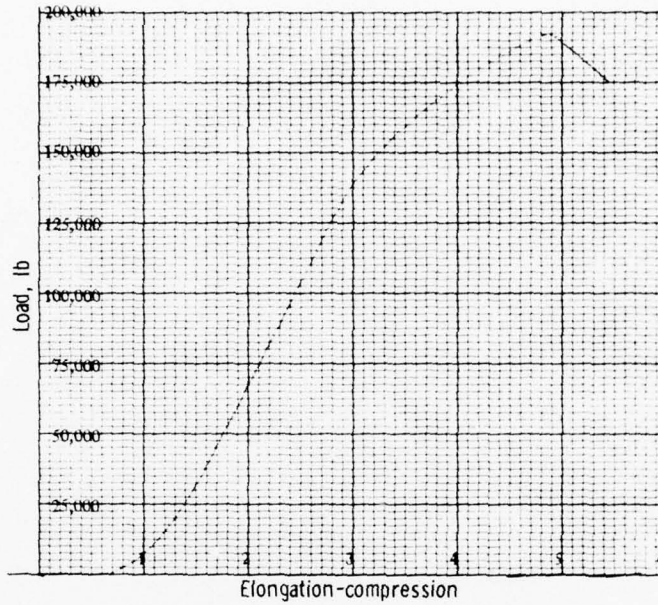


Figure D-5. Typical Load-Force Diagram

11232

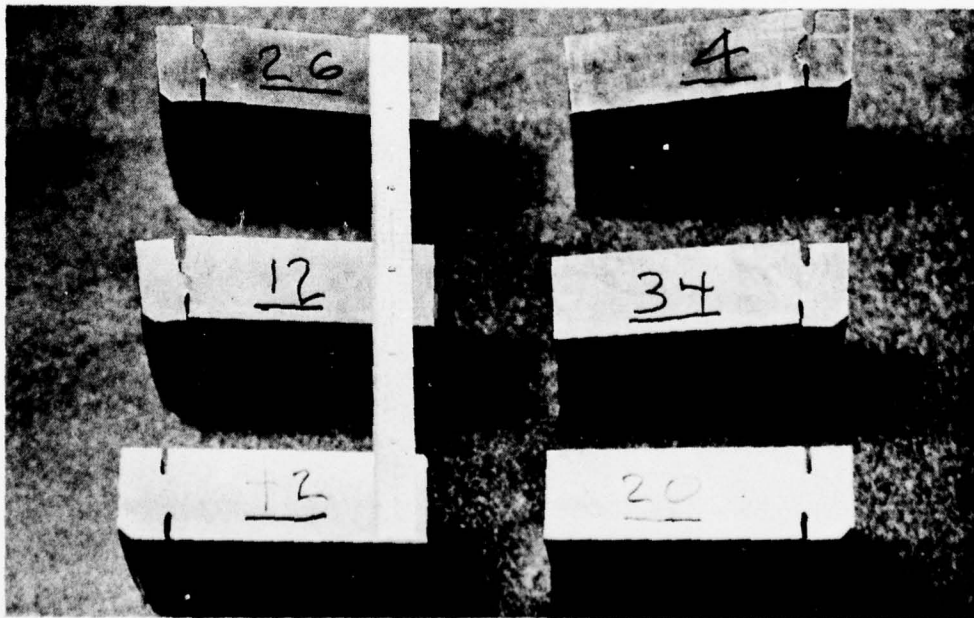


Figure D-6. Typical Test Sectors Before and After Rupture

9361-5

11185

Figure D-7 shows the failed samples with the .4- and .5-in. thickness dimension. The thinner shear samples showed more bending and translation. Figure D-8 shows the same samples relative to the position in the plate to see if direction of rolling had any effect. The 45 sectors were numbered consecutively clockwise, with the direction of rolling going through sector 1 and between 24 and 25. No strong correlation occurred. Figure D-9 compares the shear break configurations of .4-, .3- and .5-in. high rate samples. Figure D-10 shows the high and low rate samples with .35-in. thickness.

Figure D-11 shows the failure load data plotted against material thickness. The high rate samples show a lower bands of results than the low rate, and there is some tendency for failure to occur at lower loads as the number of cycles on the test fixture increases. A 3σ line was added to the curve, and the thickness was set above 2500 psi equivalent chamber pressure on this line at .46 in.



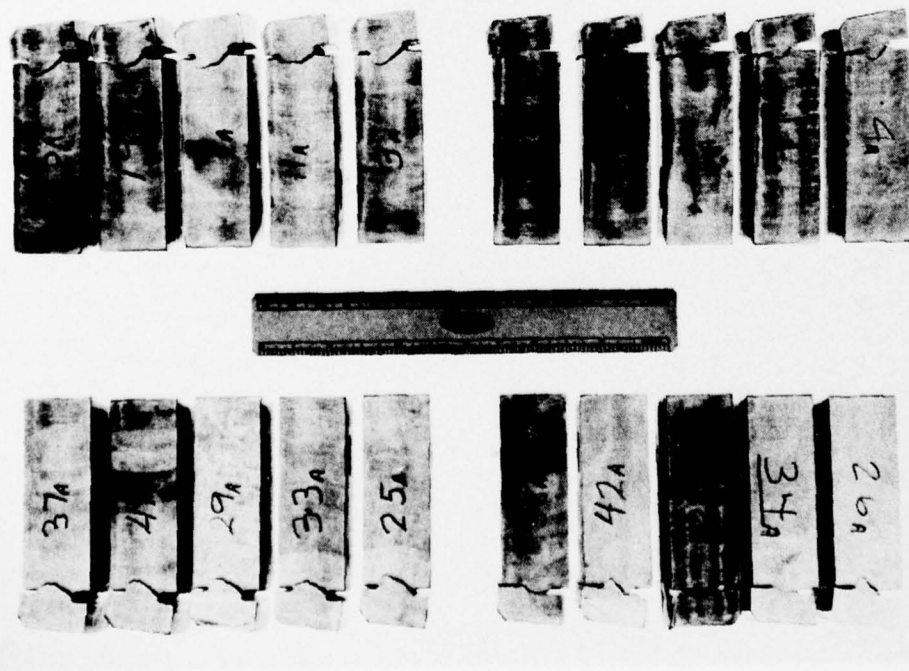


Figure D-7. Failed Samples, View 1

9361-10 11186

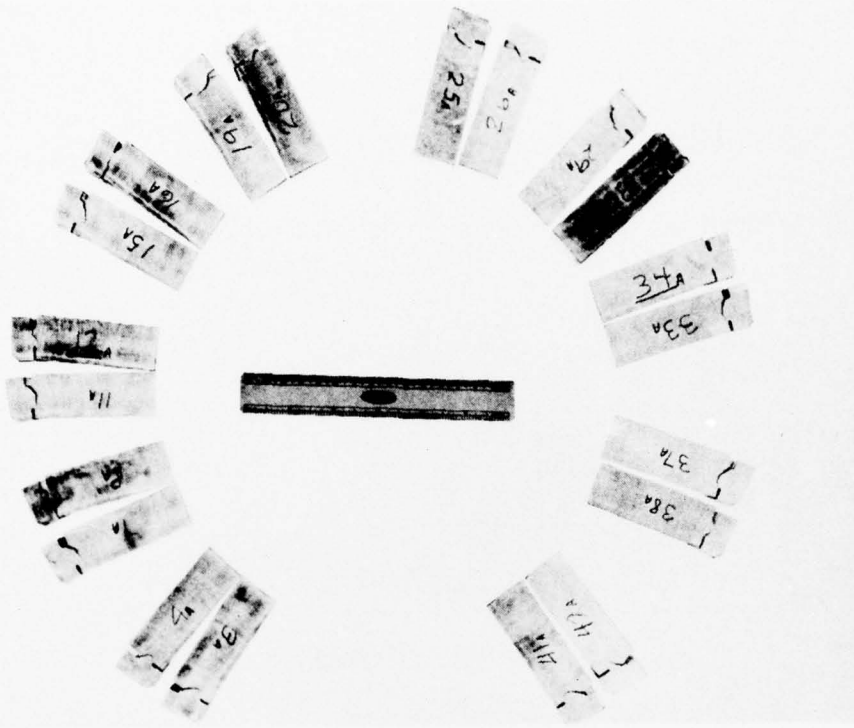


Figure D-8. Failed Samples, View 2

11187

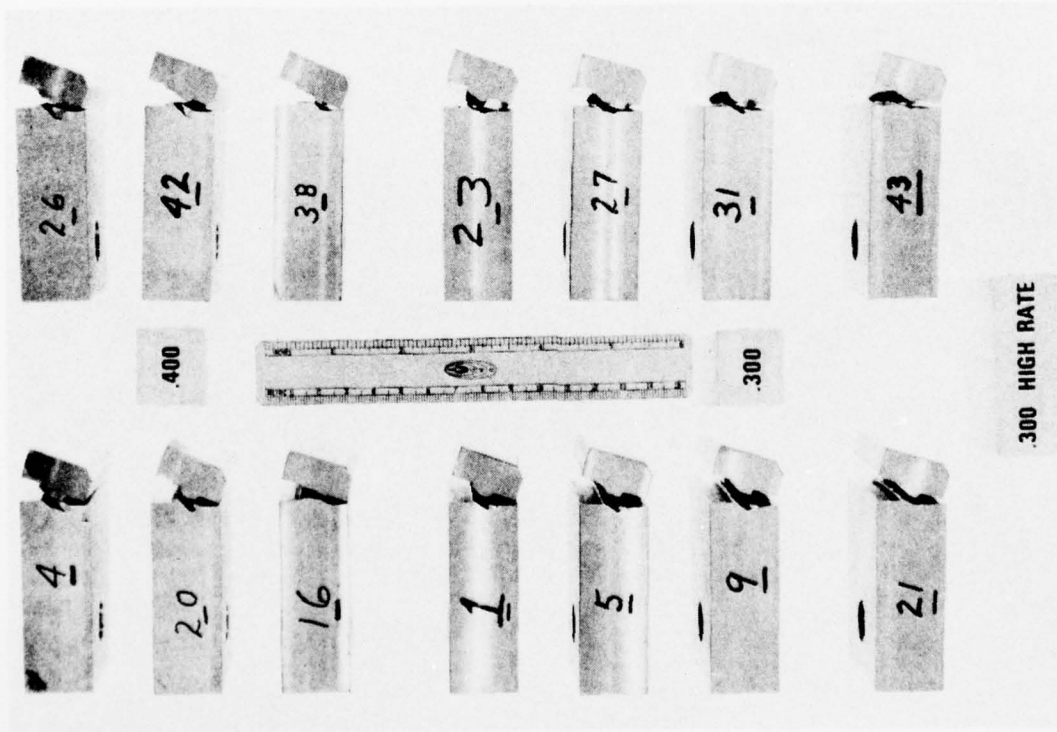


Figure D-9. Shear Break Configurations

11188

9433-1

11189

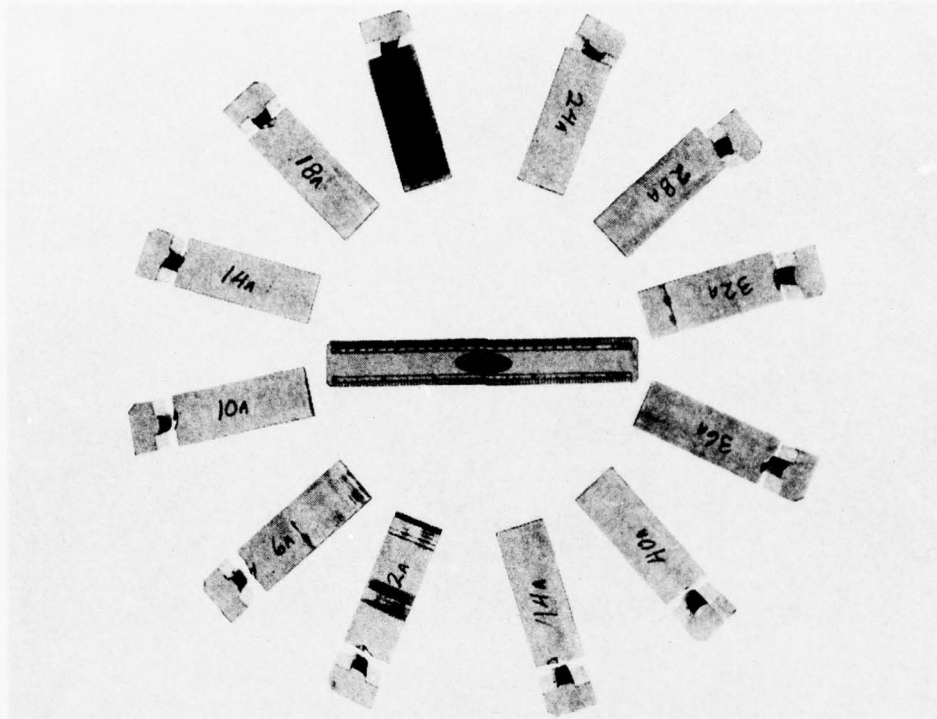


Figure D-10. High and Low Rate Samples

11189

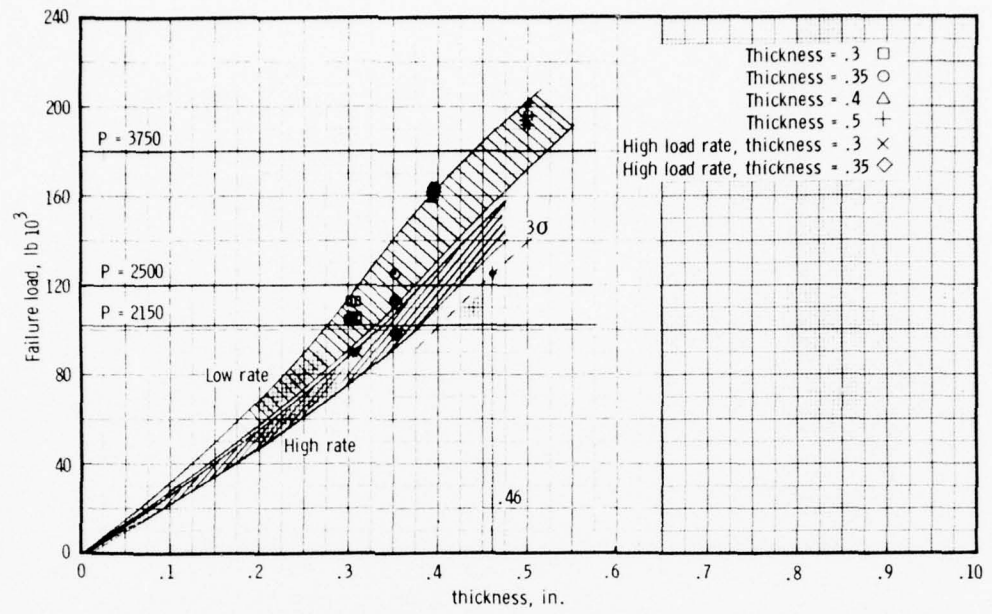


Figure D-11. Super HIPPO Shear Key Test

11190

APPENDIX E  
RPL PROCEDURE FOR LIFTING SUPER HIPPO  
PROPELLANT GRAINS

1. References:
  - a. GSOP, Section 12 for required safety equipment.
  - b. AFRPLR 127-1 for transportation of explosives.
2. Attach lift fixture C10294 to crane hook.

CAUTION

Check to insure that the crane hook does not interfere with the actuation bar.

3. Lift and position the lift fixture C10294 over the cartridge.
  - a. Assure safety latches are in up position.
  - b. Verify four lift pins are retracted (actuation arm in counter clockwise position).
4. Lower lift fixture into position on cartridge. Align index on fixture with groove on top face of cartridge.

NOTE

Fixture must be at rest on cartridge to properly align:

5. Release actuation bar spring-loaded locking pin by pulling cable. Rotate actuation arm clockwise until the four lift pins enter cartridge lift holes and actuation bar pin engages.

WARNING

Insure locking pin is fully engaged prior to lifting grain.

CAUTION

Do not force actuator bar beyond locking pin engagement position.

6. Verify lift pins are engaged  $1 \pm 1/8$  inch into cartridge holes. Lift pin is punch marked at 1 inch. If required, adjust engagement with linkage turn buckles.
7. Roll down safety grips over outside of cartridge and insert locking pins.
8. Lift cartridge as required.

9. For disengagement reverse above procedure.

CAUTION

Verify lift pins are fully disengaged before removal of fixture.  
Adjust turn buckles as required to fully withdraw lift pins.

REVIEW AND APPROVAL AUTHORIZATION

GRAIN LIFT PROCEDURE

SUPER HIPPO PROJECT NO. 305909NL

PREPARED BY: M. Gantiva  
Test Engineer

APPROVED: [Signature]  
Director of Safety

[Signature]  
Area Foreman

[Signature]  
Chief, Test and Support  
Division

COORDINATION: [Signature]  
Senior Test Engineer

#### ABBREVIATIONS

AFRPL	Air Force Rocket Propulsion Laboratories
CSD	Chemical Systems Division
ECO	engineering change order
ELSH	extended length Super HIPPO
EPDM	ethylene-propylene diene monomer
HIPPO	high internal pressure producing orifice
HTPB	hydroxy-terminated polybutadiene
IUS	interim upper stage
MEOP	maximum expected operating pressure
NBR	nitrile-butadiene rubber
SLSH	short length Super HIPPO